J Orthop Sci (2010) 15:804–809
DOI 10.1007/s00776-010-1542-5

JOURNAL OF
ORTHOPAEDIC SCIENCE

Original article

Deformity of the great toe in fibrodysplasia ossificans progressiva

YASUHARU NAKASHIMA[1,2], NOBUHIKO HAGA[2], HIROSHI KITOH[2], JUNJI KAMIZONO[2], KOJI TOZAWA[3], TAKENOBU KATAGIRI[2], TAKAFUMI SUSAMI[2], JUN-ICHI FUKUSHI[1], and YUKIHIDE IWAMOTO[1]

[1] Department of Orthopaedic Surgery, Kyushu University, 1-3-3 Maidashi, Higashi-ku, Fukuoka 812-8582, Japan
[2] Research Committee on Fibrodysplasia Ossificans Progressiva
[3] Beppu Developmental Medicine and Rehabilitation Center, Beppu, Japan

Abstract

Background. As invasive medical procedures can induce permanent heterotopic ossification in fibrodysplasia ossificans progressiva (FOP), caution should be exercised in clinical practice. The present study was conducted to examine the characteristics of the great toe deformity in patients with FOP, which may lead to an early diagnosis of this condition.

Methods. The subjects consisted of 31 feet from 16 FOP patients (8 males, 8 females) with an average age of 17.3 years (range 1–47 years) at the time of this study. Gross and radiographic findings, including the hallux valgus angles (HVA), intermetatarsal angles (IMA), and the deformity of the proximal phalanx and metatarsal bone, were examined.

Results. Of the 31 feet, 29 (93.5%) showed several degrees of great toe deformity. A shortened great toe was the typical gross finding and was observed in 20 feet (64.5%). The mean HVA and IMA were 19.7° and 8.5°, respectively; and 22 (71.0%) feet satisfied the radiographic definition of hallux valgus (HVA ≥ 20° or IMA ≥ 10°). The proximal phalanx was consistently shortened but morphologically dissimilar from case to case. The metatarsal bone was also shortened and sharpened to the medial side, deviating the proximal phalanx laterally from the metatarsal axis. Fusion between the distal and proximal phalanx occurred with advancing age. Only two feet in one patient showed no obvious deformity of the great toe.

Conclusions. A shortened great toe and hallux valgus were frequently found in patients with FOP. Shortening and sharpening of the proximal phalanx and metatarsal bone consistently existed and contributed to the great toe deformity. These findings were thought to exist from birth and may be a key to an early diagnosis.

Introduction

Fibrodysplasia ossificans progressiva (FOP) is a rare disease, affecting one in every two million people.[1,2] Starting in childhood, it involves progressive ossification of skeletal muscles, tendons, and ligaments throughout the body, leading to decreased range of joint motion and deformity in the limbs and trunk.[3–6] In the terminal phase, respiratory function is impaired due to limited movement of the thorax, and trismus is caused by a limited range of motion in the temporomandibular joint.[2,7] The overall prognosis for this disease is considered poor. Although this condition is inherited in an autosomal dominant fashion, sporadic cases are common. In 2006, mutated genes of the activin A receptor (*ACVR1*), a bone morphogenetic protein type I receptor, were reported to be responsible for this disease.[8] The identical mutation of the *ACVR1* gene was also confirmed in Japanese patients with FOP.[9,10]

"Flare-ups" develop in patients with FOP that involve swelling accompanied by warmth and pain. They usually occur during childhood and are found mainly in the spine, frequently a result of minor trauma such as a fall.[11] These flare-ups persist for 2–3 months. Although the swelling itself diminishes, the injured sites may show development of heterotopic ossification within several months. This ossification then spreads throughout the body as flare-ups occur repeatedly, resulting in gradually decreasing range of joint motion. Because some medical procedures can induce ossification, caution should be exercised in clinical practice. These procedures include resection of heterotopic ossification, biopsy, and intramuscular injection.[12] Kitterman et al. reported that unnecessary biopsies were conducted in 67% of patients, and heterotopic ossification lesions were resected in 26%. In 49% of patients, flare-ups induced by these invasive medical procedures led to permanent loss of motion.[12]

An early diagnosis is essential to avoid symptom progression through unnecessary medical procedures and to allow the earliest possible initiation of treatment.[13,14] The definitive diagnosis is currently made by identifying mutations of the *ACVR1* gene, but it also requires clinical findings suggestive of FOP. Congenital malformation

Offprint requests to: Y. Nakashima
Received: July 6, 2010 / Accepted: August 5, 2010

of the great toe is reported to be a typical finding in FOP and plays an important role in making an early diagnosis, considering that flare-ups are initiated during childhood.[13–16] This particular deformity was present in 95% of FOP cases studied by Kitterman et al. using a patient survey,[12] an incidence that was reportedly close to 100% in other publications.[13,14] After radiographically examining 15 patients with FOP, Harrison et al. noted a higher incidence of hallux valgus than is seen in healthy individuals.[15] As far as we know, there were no detailed reports on deformities of the great toe among Asian patients with FOP, and few reports fully describe the condition of the phalanges and metatarsal bones that constitute this deformity. The present study was conducted to examine the deformity of the great toe in patients with FOP both grossly and radiographically to clarify its incidence and to gather specific details regarding the affected bones.

Materials and methods

Subjects

The present study protocol was approved by our institutional review board. The subjects included 16 patients (32 feet) who were diagnosed with FOP at health care facilities where members of the Research Committee on Fibrodysplasia Ossificans Progressiva practiced. The details of the subjects are shown in Table 1. All the subjects were Japanese. There were eight males and eight females, with an average age of 17.3 years (range 1–47 years) at the time of this study. Patient 9 had had a corrective osteotomy of the left great toe when he was 7 years old. His left great toe was totally ankylosed from the metatarsal bone to the distal phalanx due to the surgical procedure, and his left toe therefore was excluded from this study. The remaining 31 feet in 16 subjects were included.

Gross findings of the great toe deformity

A shortened great toe and hallux valgus were the two major deformities evaluated (Figs. 1, 2). The tip of the great toe located proximal to the distal interphalangeal joint of the second toe was used as an indication of a shortened great toe in this study. Although the hallux valgus was defined by the radiographic measurement described below, gross findings were also described. In addition, the loss of the great toe itself or other toe was recorded.

Radiographic findings of the great toe

The hallux valgus angle (HVA) and the angle between the first and second metatarsal bones (IMA) were measured as indices of hallux valgus (Fig. 1). Hallux valgus was defined as present if the HVA was ≥20° and/or the IMA was ≥10°.[16] Because the deformity of the proximal phalanx and metatarsal bone varied among the feet, its shape and length were described. The presence or absence of fusion with the phalanges was also recorded and examined in relation to the patient's age.

Table 1. Patient demographics and morphology data

Case	Age (years)	Sex	Shortened great toe (right/left)	HVA (°) (right/left)	IMA (°) (right/left)	Fusion of proximal and distal phalanx (right/left)	Tapered distal metatarsal bone (right/left)
1	1	M	+/+	45/32	18/13	–/–	ND/ND
2	4	F	–/–	10/8	3/10	–/–	+/+
3	5	M	+/+	45/30	7/12	–/–	+/+
4	5	M	+/+	11/30	10/15	–/–	+/+
5	5	M	+/+	6/5	1/7	–/–	+/+
6	9	F	–/–	19/12	7/5	–/–	–/–
7	11	M	+/–	28/10	13/12	–/–	+/+
8	12	F	–/–	22/20	10/9	–/–	+/+
9	17	M	+/ND	25/ND	7/ND	–/ND	–/ND
10	17	F	–/–	25/14	6/9	+/+	+/+
11	22	M	+/+	20/6	10/0	+/+	+/+
12	24	F	–/–	10/13	8/7	+/+	+/+
13	27	F	+/+	28/22	11/2	+/+	+/+
14	34	M	+/+	20/7	10/2	+/+	+/–
15	37	F	+/+	30/25	10/10	+/+	+/–
16	47	F	+/+	20/15	10/10	+/+	+/–

HVA, hallux valgus angle; IMA, intermetatarsal angle; ND, not determined

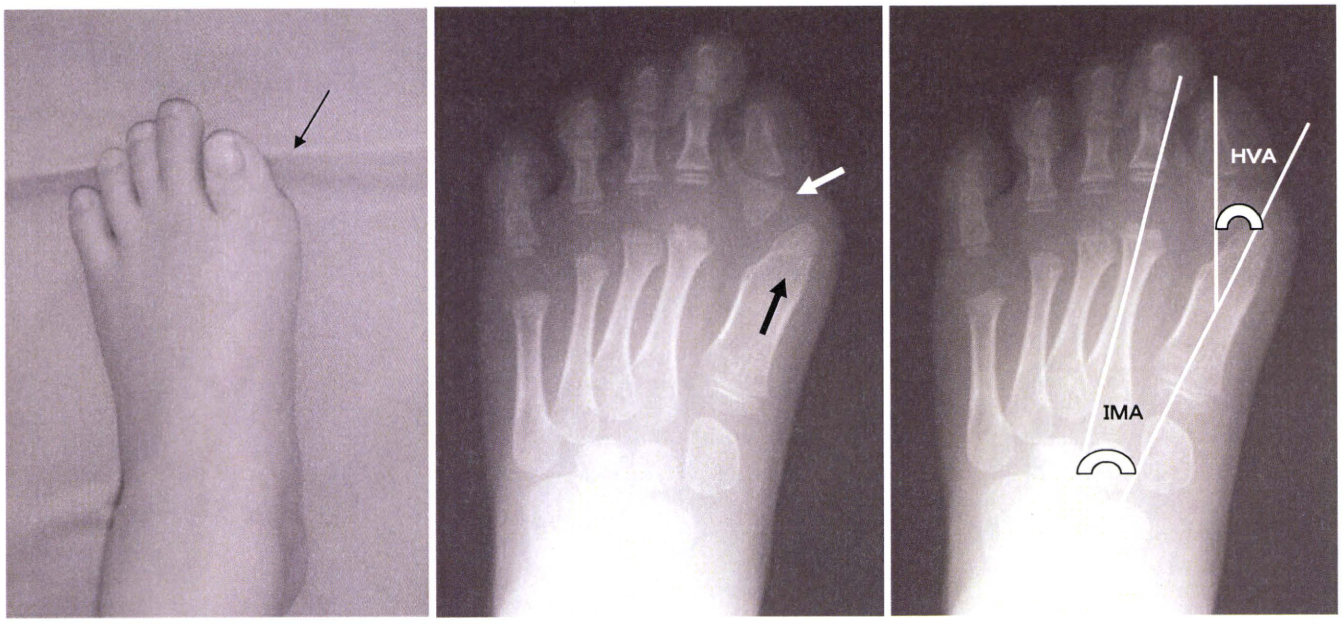

Fig. 1. Foot of a 5-year-old boy shows typical findings of fibrodysplasia ossificans progressiva (FOP). Note the shortened great toe (**a**, *arrow*) and the short and triangular proximal phalanx (**b**, *white arrow*). The metatarsal bone tapers at the distal end and deviates medially (*black arrow*). The proximal phalanx faces the lateral side of the distal metatarsal bone. **c** Hallux valgus angle (HVA) and the angle between the first and second metatarsal bones (IMA)

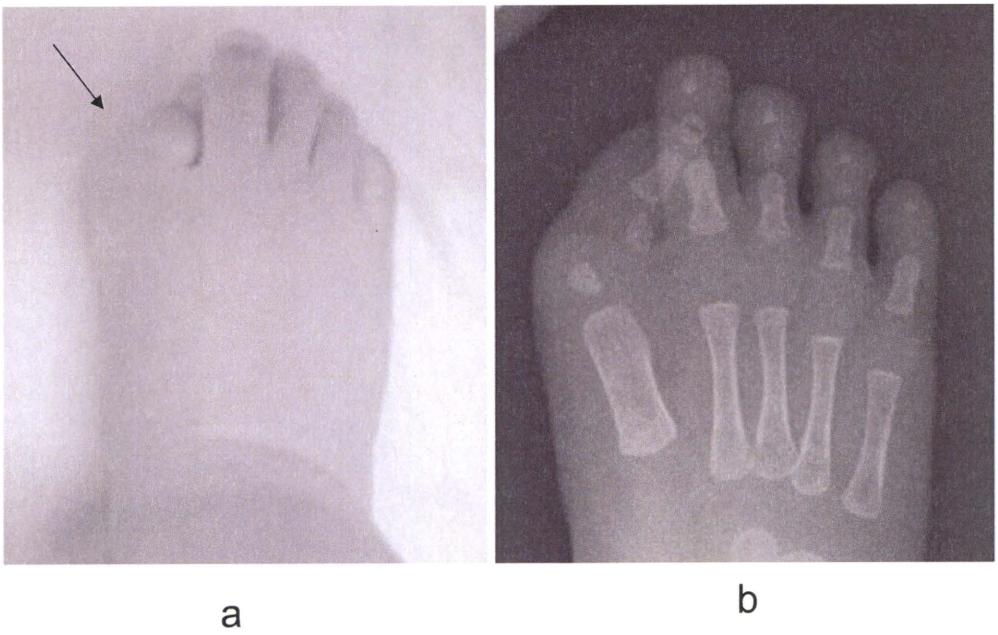

Fig. 2. **a** Note the shortened great toe with severe hallux valgus (*arrow*) in a 1-year-old boy. **b** The HVA and IMA are 45° and 18°, respectively. This case suggests the inherent deformity of the great toe in patients with FOP

Statistics

Patients were divided into two groups by the age at skeletal maturity (15 years old). Group 1 included individuals <15 years old (cases 1–8); and group 2 included those ≥15 years old (cases 9–16). The impact of age on the above-mentioned deformity of the great toe was examined by comparing these two groups using Fisher's exact test and the Mann-Whitney U-test. Significance was determined if $P < 0.05$.

Table 2. Comparison of the morphological data in groups 1 and 2

Parameter	Group 1: age <15 years (16 feet)	Group 2: age ≥15 years (15 feet)	*P*
Shortened great toe	56.3%	73.3%	0.4578
HVA[a]	20.8° ± 13.1°	18.7° ± 7.5°	0.8740
IMA[a]	9.5° ± 4.4°	7.5° ± 3.5°	0.1923
Fusion of proximal and distal phalanx	0	93.3%	<0.0001
Tapered distal metatarsal bone	75.0%	73.3%	0.6513

[a] Results are the mean ± SD

Fig. 3. Variations of the great toe deformity found in patients with FOP. **a** Triangular proximal phalanx and hallux valgus (*arrow*) in a 17-year-old boy. **b** Trapezoidal proximal phalanx and sharpened metatarsal bone without shortening or hallux valgus in a 4-year-old girl. **c** Fusion of the proximal and distal phalanx and a shortened great toe (*arrow*) in a 27-year-old woman

Results

Gross deformity of the great toe

A shortened great toe was observed in 22 of 33 feet (66.7%) (Table 1; Figs. 1, 2). Hallux valgus was observed along with the shortened great toes in most cases; five feet showed only great toe shortening. We did not detect loss of the great toe itself or of its nail in any of cases examined in this study, nor was there a loss of other toes.

Radiographic findings

The mean HVA was 19.7° (range 5°–45°). The mean IMA was 8.5° (range 2°–18°). Of the 31 feet, 22 (71.0%) exhibited hallux valgus with HVA > 20° or IMA > 10°. There were no significant differences in the HVA (20.8° vs. 18.7°) or the IMA (9.5° vs. 7.5°) between groups 1 and 2 ($P > 0.05$) (Table 2).

Deformity of the proximal phalanx was not uniform, with shapes that ranged from triangular to trapezoidal (Fig. 3). They were often short and small and were located lateral to the axis of the metatarsal bone. The first metatarsal bone was tapered at the distal end and shorter in length in 74.2% of the feet. The axis of the metatarsal bone was deviated medially, and the proximal phalanx faced the lateral side of the distal metatarsal bone, leading to the shortened great toe and hallux valgus deformity.

Fusion of the proximal and distal phalanx was observed in 14 feet (45.2%). Fusion was observed more frequently among older patients, occurring in 93.3% of feet in group 2. In contrast, no fusion was observed in the younger group ($P < 0.0001$) (Table 2).

In all, 29 feet (93.5%) in 15 patients showed several degrees of the deformities described above. Only two feet in one case (9-year-old girl) did not show any deformities at the time of this study (Fig. 4), although she showed the typical findings of FOP on her back and other joints (data not shown).

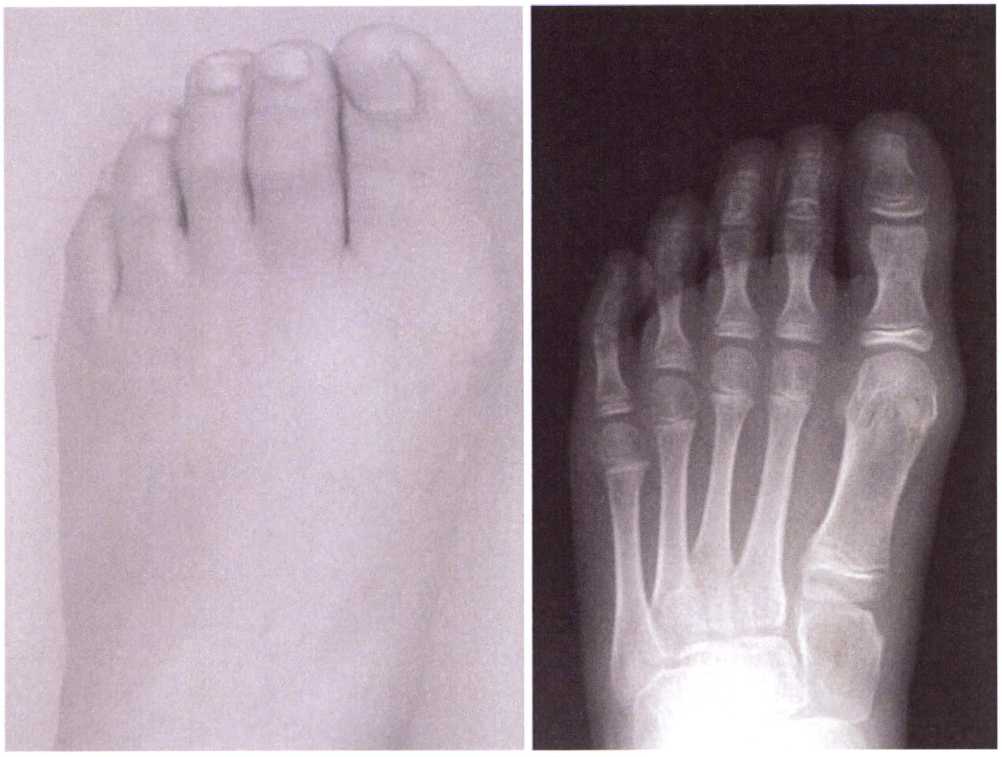

a b

Fig. 4. a, b A 9-year-old girl without the typical great toe deformity. Her foot does not show shortening or hallux valgus deformity

Discussion

In the present study, deformity of the great toe was grossly and radiographically examined in 16 Japanese patients with diagnosed FOP. In all 29 feet (93.5%) of 16 patients showed several degrees of great toe deformity. A shortened great toe was the typical gross finding and was observed in 64.5%; and 22 feet (71.0%) satisfied the radiographic definition of hallux valgus. The proximal phalanx was consistently shortened; and the metatarsal bone was sharpened to the medial side, deviating the proximal phalanx laterally. Fusion between the distal and proximal phalanx occurred with advancing age.

Because deformity of the great toe is known to be present at birth, it is important to diagnose FOP early. Kaplan et al. suggested that it is the most useful finding compared to other findings for an early diagnosis of FOP.[13] Kitterman et al. and other authors reported that deformity of the great toe was present in almost 100% of patients with FOP.[12,13] In the present study, deformities of the great toe, such as shortened length or valgus angulation, were present in 93% of cases. The presence of the deformity in a 1-year-old boy suggested the inherent condition of this deformity, and our results showed its high diagnostic value.

Deformity of the great toe comprises a deformity of the proximal phalanx and the metatarsal bone, as previously reported[15]; even so, there was a wide variation in the deformity of these bones found in the present study. The proximal phalanx was morphologically dissimilar from case to case; however, they were consistently shortened and were often located lateral to the axis of the metatarsal bones at its distal end. The metatarsal bone was also shortened and sharpened to the medial side, deviating the proximal phalanx laterally from the metatarsal axis. These deformities further exacerbated the shortening and valgus of the whole great toe.

According to Connor and Evans,[2] some deformities of the great toe often change with age. In fact, in our study, there was significant fusion of the proximal and distal phalanges in patients ≥15 years of age, whereas such a change was not common in patients <15 years in this study. Therefore, certain great toe deformities may still develop over time in the 9-year-old girl who was the only patient without apparent deformities in the present study.

Skeletal malformation in the extremities was not limited to the great toe but was also observed in thumbs from the early periods. Connor and Evans showed short thumbs due to short first metacarpals in 59% of patients and fifth-finger clinodactyly in 44%.[2] Smith et al. reported 13 patients with similar findings.[5] Among the available radiographs of three patients in our group I (younger group), all six thumbs were short without obvious angular deformity (data not shown). The first

metacarpal bones were short, and the distal and proximal phalanges had an almost normal shape, as previously reported. Three fifth fingers showed several degrees of clinodactyly. As the deformity of the upper extremity is more likely to being found, the short thumbs coupled with the deformity of the great toe may contribute the early diagnosis of FOP.

The genetic mutation associated with FOP usually involves a change in the 206th amino acid of the *ACVR1* gene, which is commonly R to H, although other mutations have been reported. Furuya et al. reported a patient with FOP whose 356th amino acid, G, was replaced by D in the *ACVR1* gene. The great toe itself was missing on both feet of this patient, as were the thumbs.[17] Thus, among mutations of the *ACVR1* gene, phenotypes can differ depending on the site of mutation. In the present study, the only patient (9-year-old girl) without deformity of the great toe had the common mutation of *ACVR1* (R206H). Further accumulation of cases is necessary to clarify the relation between these genetic mutations and phenotypes.

The primary limitation of the present study is that it was conducted as a cross-sectional study. Because the patients were not observed over time, the impact of age could only be speculated. Our findings indicated that the incidence of fusion of the proximal and distal phalanges increased with age. We therefore predict that fusion would also become more common over time in group 1. It is necessary to follow patients with serial examinations.

Conclusion

Shortening and valgus deformities of the great toe were present in most of the patients studied. The misshaped great toe consisted of a deformity of the proximal phalanx, its fusion with the distal phalanx, and deformity of the metatarsal bone. Deformity of the great toe is thought to be present at birth in patients with FOP and therefore is an important finding for an early diagnosis.

Acknowledgment. This work was supported by the project "Research on Measures for Intractable Diseases," sponsored by the Ministry of Health, Labor, and Welfare of Japan.

The authors thank Dr. Masanori Fujii for his help in preparing this manuscript.

References

1. Delatycki M, Rogers JG. The genetics of fibrodysplasia ossificans progressiva. Clin Orthop 1998;346:15–8.
2. Connor JM, Evans DA. Fibrodysplasia ossificans progressiva: the clinical features and natural history of 34 patients. J Bone Joint Surg Br 1982;64:76–83.
3. Rogers JG, Geho WB. Fibrodysplasia ossificans progressiva: a survey of forty-two cases. J Bone Joint Surg Am 1979;61: 909–14.
4. Cohen RB, Hahn GV, Tabas JA, Peeper J, Levitz CL, Sando A, et al. The natural history of heterotopic ossification in patients who have fibrodysplasia ossificans progressiva: a study of forty-four patients. J Bone Joint Surg Am 1993;75:215–9.
5. Smith R, Athanasou NA, Vipond SE. Fibrodysplasia (myositis) ossificans progressiva: clinicopathological features and natural history. Q J Med 1996;89:445–6.
6. Smith R. Fibrodysplasia (myositis) ossificans progressiva: clinical lessons from a rare disease. Clin Orthop 1998;346:7–14.
7. Vashisht R, Prosser D. Anesthesia in a child with fibrodysplasia ossificans progressiva. Paediatr Anaesth 2006;16:684–8.
8. Shore EM, Xu M, Feldman GJ, Fenstermacher DA, Cho TJ, Choi IH, et al. A recurrent mutation in the BMP type I receptor ACVR1 causes inherited and sporadic fibrodysplasia ossificans progressiva. Nat Genet 2006;38:525–7.
9. Nakajima M, Haga N, Takikawa K, Manabe N, Nishimura G, Ikegawa S. The ACVR1 617G > A mutation is also recurrent in three Japanese patients with fibrodysplasia ossificans progressiva. J Hum Genet 2007;52:473–5.
10. Fukuda T, Kohda M, Kanomata K, Nojima J, Nakamura A, Kamizono J, et al. Constitutively activated ALK2 and increased SMAD1/5 cooperatively induce bone morphogenetic protein signaling in fibrodysplasia ossificans progressiva. J Biol Chem 2009;284:7149–56.
11. Glaser DL, Rocke DM, Kaplan FS. Catastrophic falls in patients who have fibrodysplasia ossificans progressiva. Clin Orthop 1998;346:110–6.
12. Kitterman JA, Kantanie S, Rocke DM, Kaplan FS. Iatrogenic harm caused by diagnostic errors in fibrodysplasia ossificans progressiva. Pediatrics 2005;116:654–61.
13. Kaplan FS, Xu M, Glaser DL, Collins F, Connor M, Kitterman J, et al. Early diagnosis of fibrodysplasia ossificans progressiva. Pediatrics 2008;121:1295–300.
14. Kaplan FS, Le Merrer M, Glaser DL, Pignolo RJ, Goldsby RE, Kitterman JA, et al. Fibrodysplasia ossificans progressiva. Best Pract Res Clin Rheumatol 2008;22:191–205.
15. Harrison RJ, Pitcher JD, Mizel MS, Temple HT, Scully SP. The radiographic morphology of foot deformities in patients with fibrodysplasia ossificans progressiva. Foot Ankle Int 2005;26: 937–41.
16. Coughlin MJ, Jones CP. Hallux valgus: demographics, etiology, and radiographic assessment. Foot Ankle Int 2007;28:759–77.
17. Furuya H, Ikezoe K, Wang L, Ohyagi Y, Motomura K, Fujii N, et al. A unique case of fibrodysplasia ossificans progressiva with an ACVR1 mutation, G356D, other than the common mutation (R206H). Am J Med Genet A 2008;146A:459–63.

MOLECULAR ENDOCRINOLOGY

Suppression of BMP-Smad Signaling Axis-Induced Osteoblastic Differentiation by Small C-terminal Domain Phosphatase 1, a Smad Phosphatase

Shoichiro Kokabu, Satoshi Ohte, Hiroki Sasanuma, Masashi Shin, Katsumi Yoneyama, Eiko Murata, Kazuhiro Kanomata, Junya Nojima, Yusuke Ono, Tetsuya Yoda, Toru Fukuda and Takenobu Katagiri

Mol. Endocrinol. 2011 25:474-481 originally published online Jan 14, 2011; , doi: 10.1210/me.2010-0305

Suppression of BMP-Smad Signaling Axis-Induced Osteoblastic Differentiation by Small C-terminal Domain Phosphatase 1, a Smad Phosphatase

Shoichiro Kokabu, Satoshi Ohte, Hiroki Sasanuma, Masashi Shin, Katsumi Yoneyama, Eiko Murata, Kazuhiro Kanomata, Junya Nojima, Yusuke Ono, Tetsuya Yoda, Toru Fukuda, and Takenobu Katagiri

Division of Pathophysiology, Research Center for Genomic Medicine (S.K., S.O., H.S., M.S., K.Y., K.K., J.N., T.F., T.K.), and School of Medical Technology and Health, Faculty of Health and Medical Care (E.M.), Saitama Medical University, Hidaka-shi, Saitama 350-1241, Japan; Department of Oral and Maxillofacial Surgery, Faculty of Medicine (S.K., J.N., T.Y.), Saitama Medical University, Moroyama-machi, Iruma-gun, Saitama 350-0495, Japan; and King's College London, Randall Division of Cell and Molecular Biophysics (Y.O.), Guy's Campus, London SE1 1UL, UK

Bone morphogenetic proteins (BMPs) induce osteoblastic differentiation in myogenic cells via the phosphorylation of Smads. Two types of Smad phosphatases—small C-terminal domain phosphatase 1 (SCP1) and protein phosphatase magnesium-dependent 1A—have been shown to inhibit BMP activity. Here, we report that SCP1 inhibits the osteoblastic differentiation induced by BMP-4, a constitutively active BMP receptor, and a constitutively active form of Smad1. The phosphatase activity of SCP1 was required for this suppression, and the knockdown of SCP1 in myoblasts stimulated the osteoblastic differentiation induced by BMP signaling. In contrast to protein phosphatase magnesium-dependent 1A, SCP1 did not reduce the protein levels of Smad1 and failed to suppress expression of the *Id1*, *Id2*, and *Id3* genes. Runx2-induced osteoblastic differentiation was suppressed by SCP1 without affecting the transcriptional activity or phosphorylation levels of Runx2. Taken together, these findings suggest that SCP1 may inhibit the osteoblastic differentiation induced by the BMP–Smad axis via Runx2 by suppressing downstream effector(s). (*Molecular Endocrinology* 25: 474–481, 2011)

Bone morphogenetic proteins (BMPs) were originally identified as factors inducing ectopic bone formation when implanted into muscle tissues (1). BMPs inhibit the myogenic maturation of myoblasts and convert their differentiation pathway into that of the osteoblast lineage (2). BMP signaling is transduced by two different types of transmembrane serine/threonine kinase receptors termed type I and II receptors (3, 4). The BMP-bound type II receptor phosphorylates the type I receptor, and the activated BMP type I receptor in turn phosphorylates downstream substrates such as receptor-regulated Smads (R-Smads), including Smad1, Smad5, and Smad8, in addition to MAPKs such as Erk, Jnk, and p38 (5).

Smads play central roles among the downstream signaling effectors of BMP receptors. R-Smads are phosphorylated by BMP receptors on two serine residues in the Ser-X-Ser (SXS) motif at the C terminus (6–8). Replacing these serine residues with aspartic acid residues in Smad1 mimics the phosphorylated state induced by the BMP receptors (9). Phosphorylated R-Smads and the mutant Smad1 form heteromeric complexes with Smad4 and directly activate the transcription of immediate early BMP-responsive genes, including *Id1*, *Id2*, and *Id3*, within an hour (10–13). Both Osterix (Osx) and Runx2 are master regulators of osteoblast differentiation and are indirectly activated by Smads within several hours (14, 15).

ISSN Print 0888-8809 ISSN Online 1944-9917
Printed in U.S.A.

doi: 10.1210/me.2010-0305 Received July 30, 2010. Accepted December 8, 2010.
First Published Online January 14, 2011

Abbreviations: ALP, Alkaline phosphatase; BMP, bone morphogenetic protein; FOP, fibrodysplasia ossificans progressiva; OC, osteocalcin; Osx, Osterix; PPM1A, protein phosphatase magnesium-dependent 1A; R-Smad, receptor-regulated Smad; SCP, small C-terminal domain phosphatase; SXS, Ser-X-Ser.

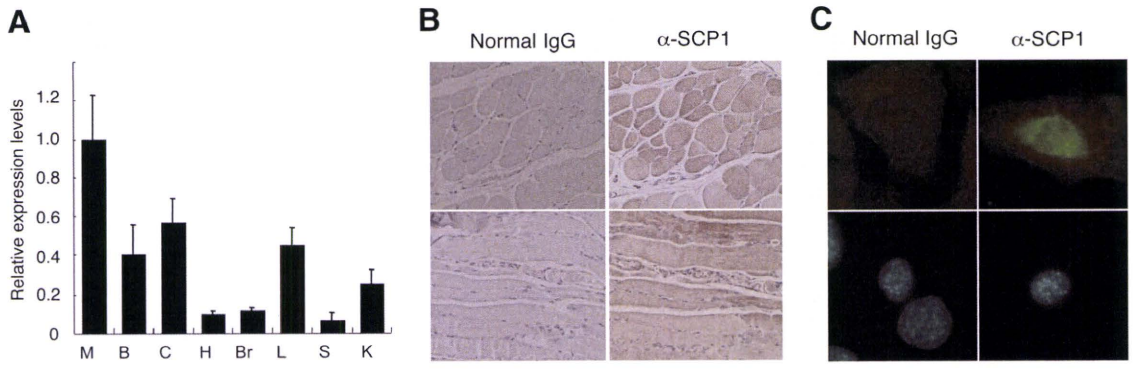

FIG. 1. SCP1 is expressed in murine skeletal muscle. A, Real-time PCR analysis of SCP1 in various murine tissues. M, skeletal muscle; B, bone; C, cartilage; H, heart; Br, brain; L, liver; S, spleen; K, kidney. B, Immunohistochemistry-based detection of SCP1 in the murine biceps femoris muscle. The cross- (*top*) and vertical (*bottom*) sections were stained with an anti-SCP1 antibody. Original magnification, ×20. C, Endogenous SCP1 in C2C12 myoblasts (*top*) and DAPI staining (*bottom*). Original magnification, ×40.

By contrast, the phosphorylation of a linker region in R-Smads by MAPKs suppresses their translocation to the nucleus and thus represses their transcriptional activity (16). Smads phosphorylated at the MAPK sites selectively bind to Smad ubiquitination regulatory factor 1, a member of the E3 ubiquitin ligase family that targets proteins for ubiquitination and proteasomal degradation (17). The phosphorylation of this linker region by MAPKs or GSK3β induces the degradation of Smad1 (18).

Two distinct types of phosphatases, small C-terminal domain phosphatases (SCPs) and protein phosphatase magnesium-dependent 1A (PPM1A), have been identified as enzymes that stimulate the dephosphorylation of Smads (19, 20). SCP1 was first identified as a phosphatase of the C-terminal domain of an RNA polymerase II subunit and has been shown to act as an evolutionarily conserved transcriptional corepressor to inhibit neuronal gene transcription in non-neuronal cells (21, 22). Through SCP3, SCP1 suppresses BMP activity by dephosphorylating the C-terminal SXS motifs in Smads (19). In addition, SCPs dephosphorylate the MAPK phosphorylation sites in the linker region of Smads (23). PPM1A suppresses TGF-β and BMP signaling by dephosphorylating the SXS motifs in Smad2/3 and Smad1 (20, 24).

We recently reported that PPM1A suppresses BMP signaling by inducing the degradation of R-Smads independently of the dephosphorylation at the SXS motif and a Smad ubiquitination regulatory factor 1–binding site in Smad1 (25). In the present study, we examined the molecular mechanisms of the inhibitory effect of SCP1 on the BMP-induced osteoblastic differentiation of myogenic cells. Similar to PPM1A, SCP1 inhibited the osteoblastic differentiation induced by BMP-4, a constitutively activated BMPR-IA, and a constitutively activated Smad1. Furthermore, knockdown of endogenous SCP1 stimulated BMP activity. The inhibitory activity of SCP1 was dependent on phosphatase activity but independent of the phosphorylation state of Smad1 at the linker region and the SXS motif. In contrast to PPM1A, SCP1 did not reduce the protein levels of Smad1 and failed to suppress the expression of the immediate early Smad-responsive genes. Moreover, Runx2-induced expression of *Osx*, *alkaline phosphatase* (*ALP*), and *osteocalcin* (*OC*) mRNAs was suppressed by SCP1. Taken together, these data suggest that SCP1 may target downstream effector(s) in addition to Smads themselves during the osteoblastic differentiation induced by BMPs.

Results

SCP1 is expressed in murine skeletal muscle and myoblasts

We analyzed the expression levels of *SCP1* in various murine tissues using real-time PCR. SCP1 mRNA was detected in all of the tissues examined, with the highest level observed in skeletal muscle (Fig. 1A). Immunohistochemical analysis indicated that the SCP1 protein was localized primarily in the fused myofibers of the biceps femoris muscle (Fig. 1B). In cultured C2C12 myoblasts, endogenous SCP1 was detected in both the nucleus and the cytoplasm, particularly in perinuclear areas of the cytoplasm (Fig. 1C).

SCP1 suppresses BMP activity via its phosphatase activity

Overexpression of SCP1 suppressed BMP-4-induced ALP activity (a typical marker of osteoblastic differentiation) in C2C12 cells (Fig. 2A) and primary myoblasts (Supplemental Fig. 1 published on The Endocrine Society's Journals Online web site at http://mend.endojournals.org/). In addition, SCP1 reduced the ALP activity induced by coexpression of a constitutively active BMPR-IA receptor and Smad1 in C2C12 cells (Fig. 2B), MC3T3-E1 cells (Fig. 2C), and primary osteoblasts (Fig. 2D). Further-

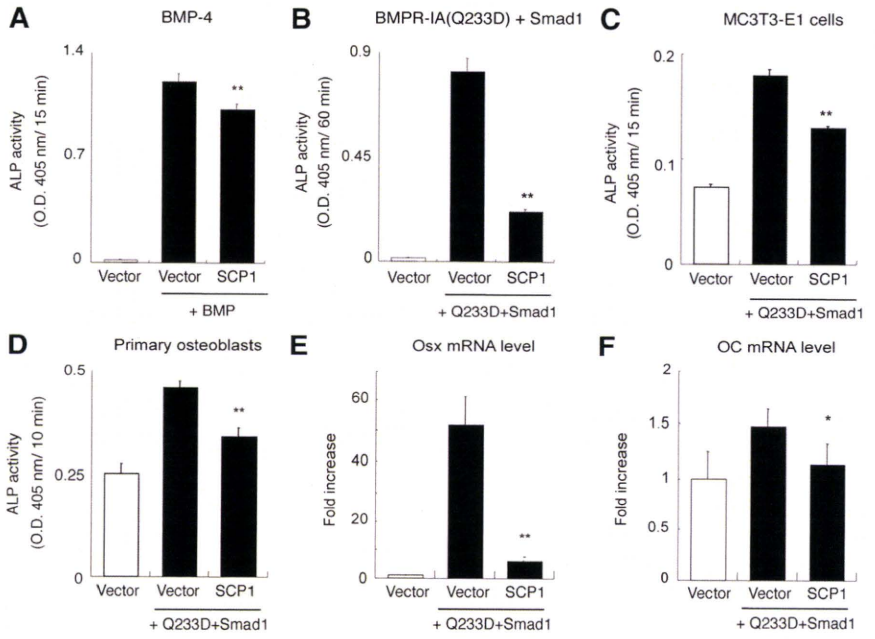

FIG. 2. SCP1 inhibits BMP signaling. SCP1 inhibited BMP signaling-induced ALP activity in C2C12 cells (A and B), MC3T3-E1 cells (C), and primary osteoblasts (D). ALP activity was activated via treatment with 100 ng/ml of BMP-4 (A) or cotransfection of BMPR-IA(Q233D) and Smad1 (B–D) in cells that had been transfected with an empty vector or SCP1. The enzyme activity of ALP was determined on d 3. E and F, SCP1 inhibited the mRNA expression of *Osx* (E) and *OC* (F), which was induced by cotransfection of BMPR-IA(Q233D) and Smad1 in C2C12 cells. The expression level of each mRNA was determined by real-time PCR on d 3. Data are shown as the mean ± SD (n = 3). *, $P < 0.05$; **, $P < 0.01$ in comparison with cells transfected with an empty vector in each group.

more, SCP1 suppressed the expression levels of osteoblastic differentiation marker genes, such as *Osx* (Fig. 2E), *OC* (Fig. 2F), *Osteonectin* (Supplemental Fig. 2A), and *parathyroid hormone receptor* (Supplemental Fig. 2B), in C2C12 cells.

Phosphorylation of Smad1 at the C terminus was dependent on BMP-4 stimulation (Fig. 3, A–C). Coexpression of wild-type SCP1, but not mutant SCP1, reduced the BMP-4-induced phosphorylation of Smad1 at the C terminus. Phospho-Smad1/5/8 proteins colocalized with mutant SCP1, but not wild-type SCP1, in both Smad1 overexpressing cells and nontransfected C2C12 cells (Fig. 3, A and B). In contrast to the C terminus, the linker region of Smad1 was simultaneously phosphorylated at Ser206 with or without of BMP-4 stimulation (Fig. 3C). Again, the linker phosphorylation was reduced by wild-type SCP1 and PPM1A but not by mutant SCP1 (Fig. 3C). However, in contrast to PPM1A, SCP1 did not decrease the protein levels of Smad1 or Smad4 in C2C12 cells as determined by Western blots (Fig. 3C and Supplemental Fig. 3).

We further examined the effects of SCP1 on a constitutively active form of Smad1, Smad1(DVD). Although this Smad1 mutant does not contain the phosphorylatable serine residues at the C terminus, it is recognized by anti–phospho-Smad1/5/8, even without BMP-4 treatment (9). In contrast to wild-type Smad1, Smad1(DVD) was localized to cells that expressed both mutant and wild-type SCP1, suggesting that SCP1 did not destroy the C-terminal structure of Smad1 (Fig. 3D). However, the Smad1(DVD)-induced ALP activity was suppressed by SCP1 (Fig. 3E). We also generated Smad1(MAPK-DVD), in which the four MAPK phosphorylation sites in the linker region of Smad1(DVD) were replaced with alanine residues. Once again, the ALP activity induced by Smad1(MAPK-DVD) was reduced by wild-type SCP1, but not by mutant SCP1 (Fig. 3F). These results suggest that SCP1 may inhibit BMP-induced osteoblastic differentiation in a manner that is dependent on its phosphatase activity and independent of the dephosphorylation of Smads at the C terminus and the linker region.

SCP1 physiologically suppresses BMP activity in myogenic cells

The transfection of C2C12 cells with SCP1-specific siRNAs reduced the protein levels of endogenous SCP1 (Fig. 4A). Furthermore, ALP activity and the levels of *Osx* mRNA induced by BMP signaling were increased in C2C12 cells that had been transfected with one of SCP1 siRNAs in comparison with cells that had been transfected with a scrambled siRNA (Fig. 4, B and C). A similar effect of SCP1-specific siRNAs was observed in primary myoblasts (Fig. 4, D and E). These findings suggest that endogenous SCP1 physiologically suppresses BMP activity in myogenic cells.

SCP1 and PPM1A target different stages of BMP-induced osteoblastic differentiation

Id genes have been identified as early BMP-responsive genes in human and murine cells (13), and the IdWT4F-luc reporter is driven by Smad-binding elements in the *Id1* gene (12). In contrast to PPM1A, SCP1 failed to suppress the IdWT4F-luc reporter activity induced by a constitutively active BMPR-IA receptor (Fig. 5A) or a constitutively active Smad1(DVD) with Smad4 (Fig. 5B). We directly compared the effects of SCP1 and PPM1A on BMP-induced gene expression using RT-PCR analysis. The expression of marker genes that are characteristic of osteoblastic differentiation, such as *Osx*, *ALP*, and *OC*, was suppressed by both SCP1 and PPM1A. By contrast,

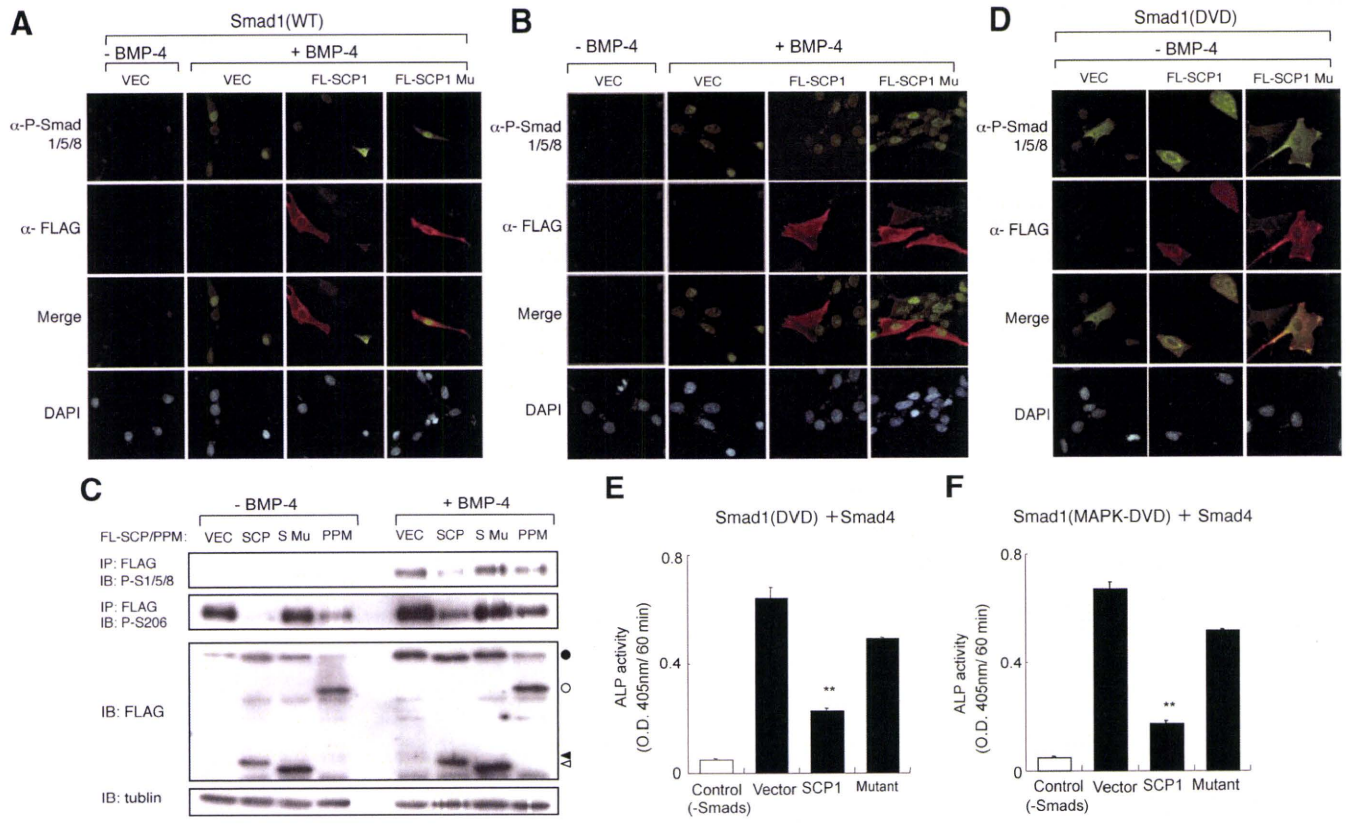

FIG. 3. Phosphatase activity is important to the inhibition of BMP signaling by SCP1. A, B, and D, Immunohistochemical analysis of phospho-Smad1/5/8 and SCP1. C2C12 cells were transfected with wild-type or mutant FLAG-SCP1 and Myc-Smad1 (A), an empty vector (B), or Smad1(DVD) (D). After treatment for 1 h with 100 ng/ml of BMP-4, the cells were double-stained with anti–phospho-Smad1/5/8 (green) and anti-FLAG (red) antibodies. C, Western blot analysis. C2C12 cells were cotransfected with wild-type or mutant FLAG-SCP1 or PPM1A along with FLAG-Smad1. After treatment for 1 h with 100 ng/ml of BMP-4, whole-cell lysates were immunoprecipitated (IP) with an anti-FLAG antibody, followed by immunoblotting (IB) with anti–phospho-Smad1/5/8 (specific for the C-terminal phosphorylation), anti–phospho-serine 206 (specific for the linker phosphorylation) in Smad1, anti-FLAG, or anti-α-tubulin antibodies. *Solid circle*, FLAG-Smad1; *open circle*, FLAG-PPM1A; *solid arrow*, wild-type FLAG-SCP1; *open arrow*, mutant FLAG-SCP1. E and F, Mutant SCP1 failed to suppress the ALP activity induced by a constitutively active form of Smad1. C2C12 cells were transfected with Smad1(DVD) (E) or Smad1(MAPK-DVD) (F) in combination with Smad4. The data are shown as the mean ± SD (n = 3). **, $P < 0.01$ in comparison with cells transfected with an empty vector in each group.

the expression of *Id1*, *Id2*, *Id3*, and *Runx2* was suppressed by PPM1A but not SCP1 (Fig. 5C).

SCP1 targets elements that are downstream of Runx2 in BMP-induced osteoblastic differentiation

Runx2 is a critical transcription factor for osteoblastic differentiation and is downstream of BMP signaling (14, 32). Overexpression of Runx2 in C2C12 cells increased the mRNA expression of genes that are related to osteoblastic differentiation, including *Osx*, *ALP*, and *OC*, without increasing the mRNA expression of *Id1*, *Id2*, and *Id3* (Fig. 6, A–D). The increased mRNA levels of *Osx*, *ALP*, and *OC* induced by Runx2 were suppressed by SCP1 but were only weakly suppressed by PPM1A (Fig. 6, A–C). SCP1 did not suppress the transcriptional activity of Runx2, as evaluated by the 6×OSE2-luc reporter, and it did not change the phospho-serine and phospho-threonine levels of Runx2 (Fig. 6, E and F; data not shown).

Discussion

In the present study, we examined the molecular mechanisms that underlie the inhibition of BMP-induced osteoblastic differentiation by SCP1. As has been previously reported (19, 23), SCP1 reduced the level of phosphorylation at the C terminus and the linker region of wild-type Smad1; this phosphatase activity was essential for the inhibition of BMP-induced osteoblastic differentiation. Interestingly, SCP1 still suppressed the ALP activity induced by constitutively active Smad1 mutants, in which the phosphorylation sites had been substituted at the C terminus and the linker region, suggesting that SCP1 may suppress BMP-induced osteoblastic differentiation by dephosphorylating unknown substrate(s) in addition to R-Smads.

We recently found that PPM1A, another Smad phosphatase, also inhibits BMP-induced osteoblastic differentiation by reducing R-Smad levels via a proteasomal path-

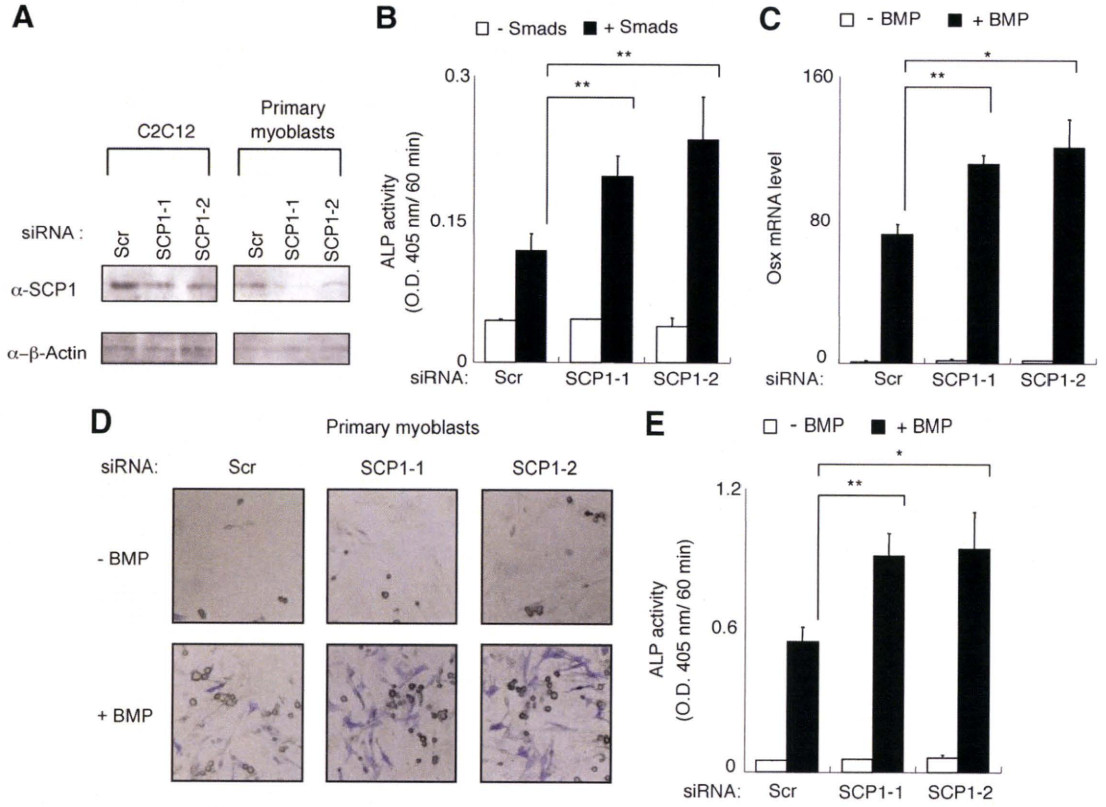

FIG. 4. Knockdown of endogenous SCP1 enhances BMP-induced osteoblastic differentiation in C2C12 cells and primary myoblasts. A, C2C12 cells (*left*) and primary myoblasts (*right*) were transfected with SCP1 siRNA or a scrambled siRNA. The level of endogenous SCP1 was examined by Western blot analysis on d 1. B, The transfection of SCP1 siRNA stimulated the ALP activity induced by Smad1(MAPK-DVD) in C2C12 cells. C, SCP1 siRNA also increased the expression of Osx mRNA induced by 100 ng/ml of BMP-4 in C2C12 cells. Real-time PCR analysis was performed on d 1. D and E, SCP1 siRNA increased the ALP activity induced by 100 ng/ml of BMP-4 in primary myoblasts. The ALP activity was stained (D) or measured (E) on d 3. The results are shown as the mean ± SD (n = 3). *, $P < 0.05$; **, $P < 0.01$.

way (25). Similarly to SCP1, the phosphatase activity of PPM1A is essential to its inhibitory effect (25). The critical difference between SCP1 and PPM1A with regard to BMP-induced osteoblastic differentiation was in their direct effects on Smads: PPM1A reduced the total Smad protein levels whereas SCP1 did not affect them. Although both SCP1 and PPM1A reduced the Smad-induced expression of genes related to osteoblastic differentiation, the expression of early BMP-responsive genes, such as *Id1*, *Id2*, and *Id3*, was suppressed by PPM1A but not SCP1. In a recent article by Knockaert *et al.* (19), SCP1 exhibited a weaker suppression of the expression of *Xvent-2*, which is a BMP-responsive gene, than did SCP2 or SCP3 in *Xenopus* embryos. It is possible that SCP1 dephosphorylates Smads after transcription of the target genes, including *Id1*. Further studies are needed to investigate this possibility. Taken together, these data suggest that PPM1A and SCP1 suppress BMP-induced osteoblastic differentiation via different molecular mechanisms: PPM1A appears to primarily target Smads and induce their degradation, whereas, in addition to Smads, SCP1 apparently targets the downstream effector(s) that

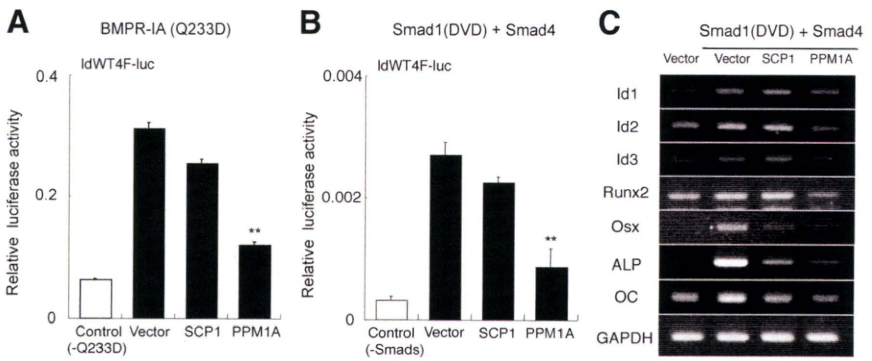

FIG. 5. Effects of SCP1 and PPM1A on the expression of early BMP-responsive genes. A and B, The effects of SCP1 and PPM1A on IdWT4F-luc reporter activity. C2C12 cells were cotransfected with SCP1, PPM1A, or an empty vector along with IdWT4F-luc and BMPR-IA(Q233D) (A) or Smad1(DVD) and Smad4 (B). The data are shown as the mean ± SD (n = 3). **, $P < 0.01$ in comparison with cells transfected with an empty vector in each group. C, The effects of SCP1 and PPM1A on the mRNA expression induced by Smad1(DVD) with Smad4. C2C12 cells were cotransfected with SCP1, PPM1A, or an empty vector, along with Smad1(DVD) and Smad4. The expression levels of the indicated mRNAs were determined by RT-PCR on d 2.

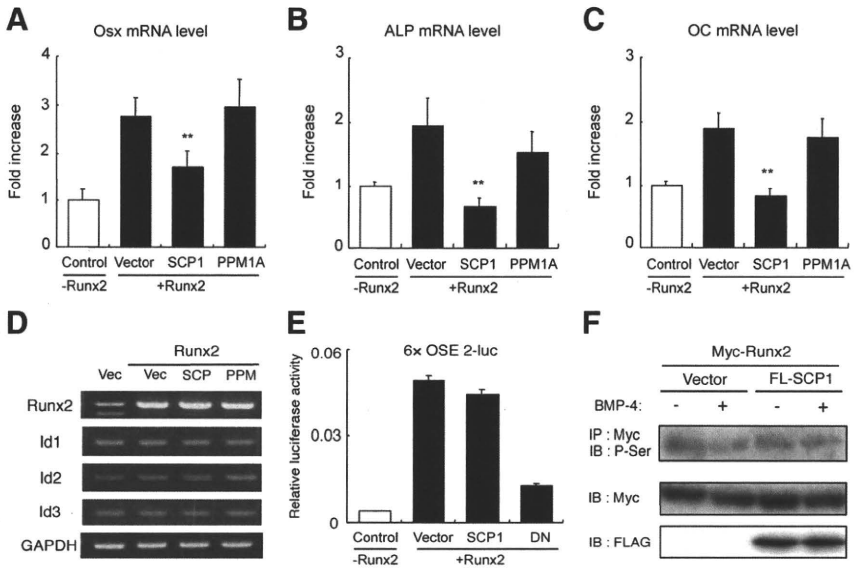

FIG. 6. SCP1 inhibits the osteoblastic differentiation induced by Runx2. A–D, The effects of SCP1 and PPM1A on Runx2-induced mRNA expression. C2C12 cells were cotransfected with SCP1, PPM1A, or an empty vector, along with Runx2. The expression levels of the indicated mRNAs were determined by real-time PCR (A–C) or RT-PCR (D) on d 2. E, SCP1 did not suppress the transcriptional activity of Runx2. C2C12 cells were cotransfected with SCP1, dominant negative Runx2 (DN), or an empty vector along with the 6×OSE2-luc reporter and Runx2. The results are shown as the mean ± SD (n = 3). **, $P < 0.01$ in comparison with cells transfected with an empty vector in each group. F, SCP1 did not change the phosphorylation levels of Runx2. C2C12 cells were cotransfected with wild-type FLAG-SCP1 or an empty vector along with Myc-Runx2. After treatment for 1 h with 100 ng/ml of BMP-4, whole-cell lysates were immunoprecipitated (IP) with an anti-Myc antibody followed by immunoblotting (IB) using anti–phospho-serine, anti-Myc, or anti-FLAG antibodies.

are required for osteoblastic differentiation without Smad degradation.

Given that Runx2 is induced by BMP signaling and that its overexpression is capable of inducing osteoblastic differentiation, Runx2 is a candidate as a critical effector in the induction of osteoblastic differentiation by the BMP–Smad pathway. Nevertheless, we found that Runx2-induced osteoblastic differentiation was suppressed by SCP1 but was only weakly suppressed by PPM1A, suggesting that PPM1A suppressed this differentiation by disrupting the synergism between Runx2 and Smads. In addition, SCP1 did not change the transcriptional activity or phosphorylation levels of Runx2, suggesting that SCP1 may inhibit effector(s) that are further downstream of Runx2 rather than Runx2 itself during suppression of BMP-induced osteoblastic differentiation. The identification of SCP1 substrates that are critical for this inhibition may shed light on the sequential cascade of osteoblastic differentiation induced by the BMP-Smad axis via Runx2.

Fibrodysplasia ossificans progressiva (FOP) is an autosomal-dominant disorder characterized by heterotopic bone formation in muscle tissues. Recently, we and others identified mutations in activin receptor-like kinase 2 that constitutively activate its kinase activity and induce the phosphorylation of R-Smads, even in the absence of BMPs (33–35). No effective treatment is available to control heterotopic bone formation in FOP patients; however, some chemical inhibitors of BMP receptors have been reported to suppress mutant activin receptor-like kinase 2 activity *in vitro* and *in vivo*. Given that SCP1 is present in skeletal muscle and myogenic cells (Fig. 1) and physiologically suppresses BMP-induced osteoblastic differentiation in myogenic cells, this phosphatase might be a novel target in preventing the heterotopic BMP-induced bone formation in muscle tissue that is typically seen in FOP patients. Enhancers of the mRNA expression and/or enzyme activity of SCP1 could be useful in the prevention of BMP-dependent bone formation *in vivo*.

In conclusion, SCP1 inhibits the osteoblastic differentiation that is induced by the BMP-Smad axis via Runx2 by suppressing downstream effector(s).

Materials and Methods

Plasmids

Plasmids encoding wild-type mouse Smad1, Smad4, mouse Osx, constitutively active BMPR-IA(Q233D), constitutively active Smad1(DVD), wild-type human PPM1A, mutant human PPM1A(R174G/D239N), and IdWT4F-luc have been described previously (12, 25). Mouse Runx2, Mouse dominant negative Runx2 (26), 6×OSE2-luc (27) were kindly provided by Dr. Toshihisa Komori (Nagasaki University). Human SCP1 (Accession number NM_182642) was obtained by a standard RT-PCR technique using Platinum Pfx DNA polymerase (Invitrogen, Carlsbad, CA) and cloned into a pcDEF3 expression vector (28). Smad1(MAPK-DVD) was generated from Smad1(DVD) by replacing the serine residues at positions 187, 195, 206, and 214 with alanine residues, using sets of mutated PCR primers. A phosphatase activity-deficient SCP1 mutant, SCP1(D96E/D98N), was generated from wild-type SCP1 by replacing aspartic acid residues at positions 96 and 98 with glutamic acid and asparagine, respectively, using sets of mutated PCR primers (23). All of the final constructs were confirmed by sequencing.

Cell culture, transfection, and ALP and luciferase assays

C2C12 mouse myoblasts and MC3T3-E1 mouse osteoblasts were maintained, treated with 100 ng/ml of BMP-4 (R&D Systems, Minneapolis, MN), and transfected with plasmids using Lipofectamine 2000 (Invitrogen), as previously described (2,

12). Primary osteoblasts were prepared from newborn mouse calvaria (29). Primary myoblasts were prepared from mouse extensor digitorum longus muscles using a single fiber isolation method (2, 30). ALP activity was measured as a marker of osteoblast differentiation on d 3 (2). Cells treated with an acetone/ethanol mixture were incubated with a substrate solution composed of 0.1 M diethanolamine, 1 mM $MgCl_2$, and 1 mg/ml p-nitrophenylphosphate. The reaction was terminated by adding 3 M NaOH, and absorbance values were measured at 405 nm (31). ALP staining was performed as previously described (2). Luciferase assays were performed using IdWT4F-luc, phRL-SV40 (Promega, Madison, WI), and 6×OSE2-luc with the Dual-Glo Luciferase Assay System (Promega), as previously described (12).

Immunohistochemistry, immunoprecipitation, and Western blot analysis

The following antibodies were used for immunohistochemistry, immunoprecipitation, and Western blot analysis: anti-FLAG (clone M2, Sigma Aldrich Chemicals, St. Louis, MO), polyclonal anti-Myc (Medical & Biological Laboratories Co., Nagoya, Japan), polyclonal anti-SCP1 (Abcam, Cambridge, MA), polyclonal anti-phosphorylated Smad1/5/8 (Cell Signaling, Beverly, MA), polyclonal anti-phosphorylated Smad1 (Ser206) (Cell Signaling), phospho-serine antibody Q5 (QIAGEN, Hilden, Germany), and phospho-threonine antibody Q7 (QIAGEN). For immunohistochemical tissue analysis, freshly isolated mouse biceps femoris muscle tissue was immediately fixed in 4% paraformaldehyde in PBS and embedded in paraffin. Vertical and cross sections 6 to 8 μm thick were deparaffinized in xylene and rehydrated with graded ethanol. Sections were incubated for 1 h with peroxidase-labeled secondary antibodies. Diaminobenzidine served as the peroxidase substrate. For fluorescent immunohistochemical analysis, target proteins were visualized using an Alexa488- or Alexa594-conjugated secondary antibody (Invitrogen). ABZ-9000 (Keyence, Tokyo, Japan) microscope was used for these analyses. The target proteins were immunoprecipitated for 1 h at 4 C using anti-FLAG M2-agarose (Sigma) or anti–c-Myc agarose beads (Sigma). For Western blot analyses, the target proteins were detected using a horseradish peroxidase–conjugated anti-mouse or anti-rabbit IgG antibody (GE Healthcare UK Ltd, Buckinghamshire, England).

Reverse transcription PCR and real-time PCR analysis

Total RNA was isolated from C2C12 cells using Trizol (Invitrogen) and then reverse-transcribed into cDNA using Superscript III (Invitrogen). The cDNA was amplified by PCR using specific primers for murine *SCP1*, *Id1*, *Id2*, *Id3*, *Runx2*, *Osx*, *ALP*, *OC*, *Osteonectin*, *parathyroid hormone receptor*, *GAPDH*, *Atp5f1*, and *Ywhaz* (TaKaRa, Ohtsu, Japan). The last three genes were used as controls. SYBR green–based real-time PCR was performed in a 96-well plate format using SYBR Premix Ex Taq (TaKaRa) with a Thermal Cycler Dice Real-Time system TP800 (TaKaRa).

RNAi transfection

GeneSolution siRNA oligonucleotides were designed against murine *SCP1* (Mm_Ctdsp1_7, QIAGEN), and a scrambled RNAi was used as a negative control (Invitrogen). Cells were transfected with 20 nM siRNA using Lipofectamine 2000 according to the manufacturer's instructions (Invitrogen).

Statistical analysis

Comparisons were made using an unpaired Student's t test; the results are shown as means ± SD. Statistical significance is indicated as $^{*}P < 0.05$ and $^{**}P < 0.01$.

Acknowledgments

We thank members of the Division of Pathophysiology, Research Center for Genomic Medicine, Saitama Medical University, for their participation in valuable discussions. We are grateful to Dr. T. Komori for kindly providing us with the mouse Runx2, Runx2 dominant negative form expression plasmid, and OSE2-luc reporter plasmid.

Address all correspondence and requests for reprints to: Takenobu Katagiri, Division of Pathophysiology, Research Center for Genomic Medicine, Saitama Medical University, 1397-1 Yamane, Hidaka-shi, Saitama 350-1241, Japan. E-mail: katagiri@saitama-med.ac.jp.

This work was supported in part by Health and Labor Sciences Research Grants for Research on Measures for Intractable Research from the Ministry of Health, Labor, and Welfare of Japan (to T.K.); grants-in-aid from the Ministry of Education, Culture, Sports, Science, and Technology of Japan (to T.F., S.O., and T.K.); a grant-in-aid from the Takeda Science Foundation (to T.K.); and a grant-in-aid for "Support Project of Strategic Research Center in Private Universities" from the Ministry of Education, Culture, Sports, Science, and Technology (MEXT) to Saitama Medical University Research Center for Genomic Medicine (to T.K.). S.K. was a recipient of the Saitama Medical University Research Fellowship.

Disclosure Summary: The authors have nothing to declare.

References

1. **Urist MR** 1965 Bone: formation by autoinduction. Science 150: 893–899
2. **Katagiri T, Yamaguchi A, Komaki M, Abe E, Takahashi N, Ikeda T, Rosen V, Wozney JM, Fujisawa-Sehara A, Suda T** 1994 Bone morphogenetic protein-2 converts the differentiation pathway of C2C12 myoblasts into the osteoblast lineage. J Cell Biol 127:1755–1766
3. **Wan M, Cao X** 2005 BMP signaling in skeletal development. Biochem Biophys Res Commun 328:651–657
4. **Miyazono K, Maeda S, Imamura T** 2005 BMP receptor signaling: transcriptional targets, regulation of signals, and signaling cross-talk. Cytokine Growth Factor Rev 16:251–263
5. **Katagiri T, Suda T, Miyazono K** 2008 The bone morphogenetic proteins. In Derynck R, Miyazono K, eds. TGF-β family. New York: Cold Spring Harbor Press, 121–149
6. **Hoodless PA, Haerry T, Abdollah S, Stapleton M, O'Connor MB, Attisano L, Wrana JL** 1996 MADR1, a MAD-related protein that functions in BMP2 signaling pathways. Cell 85:489–500
7. **Chen Y, Bhushan A, Vale W** 1997 Smad8 mediates the signaling of the ALK-2 [corrected] receptor serine kinase. Proc Natl Acad Sci USA 94:12938–12943
8. **Nishimura R, Kato Y, Chen D, Harris SE, Mundy GR, Yoneda T** 1998 Smad5 and DPC4 are key molecules in mediating BMP-2-

induced osteoblastic differentiation of the pluripotent mesenchymal precursor cell line C2C12. J Biol Chem 273:1872–1879
9. Nojima J, Kanomata K, Takada Y, Fukuda T, Kokabu S, Ohte S, Takada T, Tsukui T, Yamamoto TS, Sasanuma H, Yoneyama K, Ueno N, Okazaki Y, Kamijo R, Yoda T, Katagiri T 2010 Dual roles of smad proteins in the conversion from myoblasts to osteoblastic cells by bone morphogenetic proteins. J Biol Chem 285:15577–15586
10. López-Rovira T, Chalaux E, Massagué J, Rosa JL, Ventura F 2002 Direct binding of Smad1 and Smad4 to two distinct motifs mediates bone morphogenetic protein-specific transcriptional activation of Id1 gene. J Biol Chem 277:3176–3185
11. Liu CJ, Ding B, Wang H, Lengyel P 2002 The MyoD-inducible p204 protein overcomes the inhibition of myoblast differentiation by Id proteins. Mol Cell Biol 22:2893–2905
12. Katagiri T, Imada M, Yanai T, Suda T, Takahashi N, Kamijo R 2002 Identification of a BMP-responsive element in Id1, the gene for inhibition of myogenesis. Genes Cells 7:949–960
13. Hollnagel A, Oehlmann V, Heymer J, Rüther U, Nordheim A 1999 Id genes are direct targets of bone morphogenetic protein induction in embryonic stem cells. J Biol Chem 274:19838–19845
14. Ducy P, Zhang R, Geoffroy V, Ridall AL, Karsenty G 1997 Osf2/Cbfa1: a transcriptional activator of osteoblast differentiation. Cell 89:747–754
15. Nakashima K, Zhou X, Kunkel G, Zhang Z, Deng JM, Behringer RR, de Crombrugghe B 2002 The novel zinc finger-containing transcription factor osterix is required for osteoblast differentiation and bone formation. Cell 108:17–29
16. Kretzschmar M, Doody J, Massagué J 1997 Opposing BMP and EGF signalling pathways converge on the TGF-beta family mediator Smad1. Nature 389:618–622
17. Zhu H, Kavsak P, Abdollah S, Wrana JL, Thomsen GH 1999 A SMAD ubiquitin ligase targets the BMP pathway and affects embryonic pattern formation. Nature 400:687–693
18. Fuentealba LC, Eivers E, Ikeda A, Hurtado C, Kuroda H, Pera EM, De Robertis EM 2007 Integrating patterning signals: Wnt/GSK3 regulates the duration of the BMP/Smad1 signal. Cell 131:980–993
19. Knockaert M, Sapkota G, Alarcón C, Massagué J, Brivanlou AH 2006 Unique players in the BMP pathway: small C-terminal domain phosphatases dephosphorylate Smad1 to attenuate BMP signaling. Proc Natl Acad Sci USA 103:11940–11945
20. Lin X, Duan X, Liang YY, Su Y, Wrighton KH, Long J, Hu M, Davis CM, Wang J, Brunicardi FC, Shi Y, Chen YG, Meng A, Feng XH 2006 PPM1A functions as a Smad phosphatase to terminate TGFβ signaling. Cell 125:915–928
21. Yeo M, Lin PS, Dahmus ME, Gill GN 2003 A novel RNA polymerase II C-terminal domain phosphatase that preferentially dephosphorylates serine 5. J Biol Chem 278:26078–26085
22. Yeo M, Lee SK, Lee B, Ruiz EC, Pfaff SL, Gill GN 2005 Small CTD phosphatases function in silencing neuronal gene expression. Science 307:596–600
23. Sapkota G, Knockaert M, Alarcón C, Montalvo E, Brivanlou AH, Massagué J 2006 Dephosphorylation of the linker regions of Smad1 and Smad2/3 by small C-terminal domain phosphatases has distinct outcomes for bone morphogenetic protein and transforming growth factor-beta pathways. J Biol Chem 281:40412–40419
24. Duan X, Liang YY, Feng XH, Lin X 2006 Protein serine/threonine phosphatase PPM1A dephosphorylates Smad1 in the bone morphogenetic protein signaling pathway. J Biol Chem 281:36526–36532
25. Kokabu S, Nojima J, Kanomata K, Ohte S, Yoda T, Fukuda T, Katagiri T 2010 Protein phosphatase magnesium-dependent 1A-mdiated inhibition of BMP signaling is independent of Smad dephosphorylation. J Bone Miner Res 25:653–660
26. Maruyama Z, Yoshida CA, Furuichi T, Amizuka N, Ito M, Fukuyama R, Miyazaki T, Kitaura H, Nakamura K, Fujita T, Kanatani N, Moriishi T, Yamana K, Liu W, Kawaguchi H, Komori T 2007 Runx2 determines bone maturity and turnover rate in postnatal bone development and is involved in bone loss in estrogen deficiency. Dev Dyn 236:1876–1890
27. Ducy P, Karsenty G 1995 Two distinct osteoblast-specific cis-acting elements control expression of a mouse osteocalcin gene. Mol Cell Biol 15:1858–1869
28. Goldman LA, Cutrone EC, Kotenko SV, Krause CD, Langer JA 1996 Modifications of vectors pEF-BOS, pcDNA1 and pcDNA3 result in improved convenience and expression. Biotechniques 21:1013–1015
29. Komaki M, Katagiri T, Suda T 1996 Bone morphogenetic protein-2 does not alter the differentiation pathway of committed progenitors of osteoblasts and chondroblasts. Cell Tissue Res 284:9–17
30. Ono Y, Boldrin L, Knopp P, Morgan JE, Zammit PS 2010 Muscle satellite cells are a functionally heterogeneous population in both somite-derived and branchiomeric muscles. Dev Biol 337:29–41
31. Kodaira K, Imada M, Goto M, Tomoyasu A, Fukuda T, Kamijo R, Suda T, Higashio K, Katagiri T 2006 Purification and identification of a BMP-like factor from bovine serum. Biochem Biophys Res Commun 345:1224–1231
32. Lee KS, Kim HJ, Li QL, Chi XZ, Ueta C, Komori T, Wozney JM, Kim EG, Choi JY, Ryoo HM, Bae SC 2000 Runx2 is a common target of transforming growth factor beta1 and bone morphogenetic protein 2, and cooperation between Runx2 and Smad5 induces osteoblast-specific gene expression in the pluripotent mesenchymal precursor cell line C2C12. Mol Cell Biol 20:8783–8792
33. Fukuda T, Kohda M, Kanomata K, Nojima J, Nakamura A, Kamizono J, Noguchi Y, Iwakiri K, Kondo T, Kurose J, Endo KI, Awakura T, Fukushi J, Nakashima Y, Chiyonobu T, Kawara A, Nishida Y, Wada I, Akita M, Komori T, Nakayama K, Nanba A, Maruki Y, Yoda T, Tomoda H, Yu PB, Shore EM, Kaplan FS, Miyazono K, Matsuoka M, Ikebuchi K, Akira O, Oda H, Jimi E, Owan I, Okazaki Y, Katagiri T 2009 Constitutively activated ALK2 and increased smad1/5 cooperatively induce BMP signaling in fibrodysplasia ossificans progressiva. J Biol Chem 284:7149–7156
34. Fukuda T, Kanomata K, Nojima J, Kokabu S, Akita M, Ikebuchi K, Jimi E, Komori T, Maruki Y, Matsuoka M, Miyazono K, Nakayama K, Nanba A, Tomoda H, Okazaki Y, Ohtake A, Oda H, Owan I, Yoda T, Haga N, Furuya H, Katagiri T 2008 A unique mutation of ALK2, G356D, found in a patient with fibrodysplasia ossificans progressiva is a moderately activated BMP type I receptor. Biochem Biophys Res Commun 377:905–909
35. Shore EM, Xu M, Feldman GJ, Fenstermacher DA, Cho TJ, Choi IH, Connor JM, Delai P, Glaser DL, LeMerrer M, Morhart R, Rogers JG, Smith R, Triffitt JT, Urtizberea JA, Zasloff M, Brown MA, Kaplan FS 2006 A recurrent mutation in the BMP type I receptor ACVR1 causes inherited and sporadic fibrodysplasia ossificans progressiva. Nat Genet 38:525–527

Novel and recurrent *TRPV4* mutations and their association with distinct phenotypes within the TRPV4 dysplasia family

J Dai,[1,2] O-H Kim,[3] T-J Cho,[4] M Schmidt-Rimpler,[5] H Tonoki,[6] K Takikawa,[7] N Haga,[7,8] K Miyoshi,[7,9] H Kitoh,[10] W-J Yoo,[4] I-H Choi,[4] H-R Song,[11] D-K Jin,[12] H-T Kim,[13] H Kamasaki,[14] P Bianchi,[15] G Grigelioniene,[16] S Nampoothiri,[17] M Minagawa,[18] S-i Miyagawa,[19] T Fukao,[20] C Marcelis,[21] M C E Jansweijer,[22] R C M Hennekam,[23] F Bedeschi,[24] A Mustonen,[25] Q Jiang,[2] H Ohashi,[26] T Furuichi,[1] S Unger,[5] B Zabel,[5] E Lausch,[5] A Superti-Furga,[5] G Nishimura,[27] S Ikegawa[1]

► Additional figures and tables are published online only. To view these files please visit the journal online (http://jmg.bmj.com).

For numbered affiliations see end of article.

Correspondence to
Shiro Ikegawa, Laboratory for Bone and Joint Diseases, Center for Genomic Medicine, 4-6-1 Shirokane-dai, Minato-ku, Tokyo 108-8639, Japan;
sikegawa@ims.u-tokyo.ac.jp

Received 27 November 2009
Revised 26 January 2010
Accepted 1 February 2010
Published Online First
24 June 2010

ABSTRACT

Background Mutations in *TRPV4*, a gene that encodes a Ca^{2+} permeable non-selective cation channel, have recently been found in a spectrum of skeletal dysplasias that includes brachyolmia, spondylometaphyseal dysplasia, Kozlowski type (SMDK) and metatropic dysplasia (MD). Only a total of seven missense mutations were detected, however. The full spectrum of *TRPV4* mutations and their phenotypes remained unclear.
Objectives and methods To examine *TRPV4* mutation spectrum and phenotype–genotype association, we searched for *TRPV4* mutations by PCR-direct sequencing from genomic DNA in 22 MD and 20 SMDK probands.
Results *TRPV4* mutations were found in all but one MD subject. In total, 19 different heterozygous mutations were identified in 41 subjects; two were recurrent and 17 were novel. In MD, a recurrent P799L mutation was identified in nine subjects, as well as 10 novel mutations including F471del, the first deletion mutation of *TRPV4*. In SMDK, a recurrent R594H mutation was identified in 12 subjects and seven novel mutations. An association between the position of mutations and the disease phenotype was also observed. Thus, P799 in exon 15 is a hot codon for MD mutations, as four different amino acid substitutions have been observed at this codon; while R594 in exon 11 is a hotspot for SMDK mutations.
Conclusion The *TRPV4* mutation spectrum in MD and SMDK, which showed genotype–phenotype correlation and potential functional significance of mutations that are non-randomly distributed over the gene, was presented in this study. The results would help diagnostic laboratories establish efficient screening strategies for genetic diagnosis of the *TRPV4* dysplasia family diseases.

Metatropic dysplasia (MD; OMIM 156530) is a severe skeletal dysplasia. "Metatropic" is derived from the Greek and refers to the age-dependent evolution of body proportion in MD, changing from short limb at birth to short trunk in childhood as a result of progressive kyphoscoliosis.[1] Affected individuals present with narrow thorax, prominent joints and occasionally tail-like coccygeal appendage (caudal tail). The radiological hallmarks of MD include narrow thoracic cage with short ribs, severe platyspondyly with elongated vertebral bodies, flared ilia with horizontal acetabula and occasionally supra-acetabular notches and marked metaphyseal enlargement of the long bones, leading to a dumbbell appearance (figure 1).[2] MD has so far been considered to be genetically heterogeneous. While the majority was felt to be autosomal dominant, a subset of patients with severe phenotypes was presumed to be inherited as autosomal recessive.[3]

Spondylometaphyseal dysplasia, Kozlowski type (SMDK; OMIM 1842522), is an autosomal dominant skeletal dysplasia characterised by short trunk with platyspondyly and metaphyseal dysplasia (metaphyseal irregularity and flaring) of the long bones (figure 2).[4 5] Progressive kyphoscoliosis is common, and the ilium is broad and occasionally flared. A diagnostic skeletal alteration of SMDK is overfaced pedicles that refer to broadened vertebral bodies extending beyond pedicles on antero-posterior radiograph of the spine (figure 2A).

Brachyolmia (BO) is a heterogeneous group of skeletal dysplasias characterised by short trunk and general platyspondyly without significant epiphysial, metaphyseal and diaphyseal changes in the long bones. Based on the mode of inheritance and radiographic features, three types have been described.[6] The autosomal dominant form of BO (OMIM 113500) shows platyspondyly that is particularly severe in the cervical spine, overfaced pedicles and broad ilia. These features resemble those of SMDK.

Autosomal dominant MD, SMDK and autosomal dominant BO are caused by heterozygous mutations in the gene encoding TRPV4 (transient receptor potential cation channel, subfamily V, member 4). TRPV4 is a calcium permeable nonselective cation channel.[7] Human TRPV4 is a protein of 871 amino-acids composed by a proline-rich region, six ankyrin (ANK) repeats, six transmembrane (TM) domains and a calmodulin-binding domain (figure 3). A putative cation-permeable pore is located between the fifth and sixth TM domains.[8] TRPV4 is activated by a variety of physical and chemical stimuli, including heat, mechano-stimuli, endogenous substances such as arachidonic acid and synthetic alpha-phorbol derivatives. TRPV4 is involved in many different cellular functions; it has an important role in differentiation of chondrocytes and terminal differentiation of osteoclasts via calcium influx.[9 10]

J Med Genet 2010;**47**:704–709. doi:10.1136/jmg.2009.075358

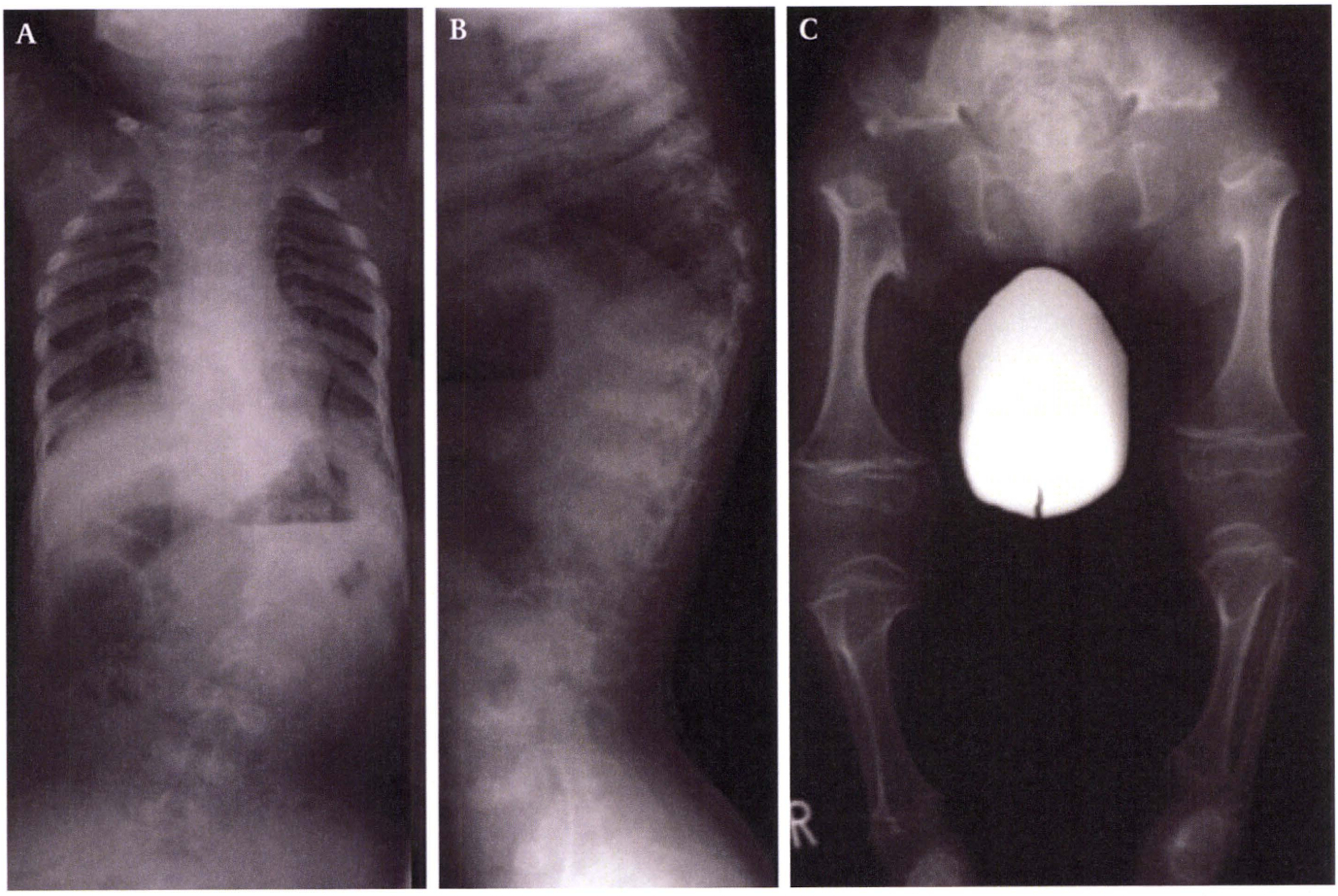

Figure 1 Radiographs of metatropic dysplasia (M8). (A) AP (antero-posterior) view of trunk, (B) lateral view of the thoracolumbar spine and (C) AP view of the lower extremities at age 3 years. There are thoracolumbar kyphoscoliosis, severe platyspondyly with overfaced pedicles and flared ilia with supra-acetabular notches. Significantly flared metaphyses of the long bones present a dumbbell deformity. Epiphysial ossification of the proximal femora is significantly retarded.

Through linkage analysis followed by a candidate gene approach, Rock *et al* identified two *TRPV4* mutations in autosomal dominant BO.[11] Because of radiological similarities between BO and SMDK, Krakow *et al* subsequently tested *TRPV4* in patients with SMDK and found three different heterozygous mutations. Then, because of radiographic similarities between MD and SMDK, they further examined *TRPV4* and found two mutations in autosomal dominant MD.[12] Thus, *TRPV4* is the causative gene of a spectrum of disorders that constitute a bone dysplasia family including autosomal dominant BO, SMDK and autosomal dominant MD. However, because only seven distinct mutations have been reported so far (three in SMDK and two in BO and MD, respectively)[11 12] (figure 3), the spectrum of *TRPV4* mutation remains unclear, as well as the range of phenotypes caused by *TRPV4* mutations.

To further evaluate these questions, we searched for *TRPV4* mutations in a total of 42 families with MD and SMDK. We detected 19 kinds of heterozygous mutations in 41 patients and found two mutational hotspots in *TRPV4*. We also found an association between location of mutations and disease phenotype.

SUBJECTS AND METHODS

Patients

MD and SMDK patients were enrolled from the participating institutions. The study was approved by the ethical committee of RIKEN and participating institutions and informed consent was obtained from all subjects. Clinical assessments for the patients were performed by their clinicians (Supplementary Table 1). The radiological features were reviewed by two pediatric radiologists (O.K. and G.N.) and by a paediatrician and a geneticist (A.S.-F. and S.U.) separately, and then discussed to consensus conclusion (supplementary Table 2).

The radiographic criteria for MD included wafer-like thin or diamond-shaped vertebral bodies in infancy and marked platyspondyly with progressive spinal deformities (scoliosis and/or kyphosis) in childhood (figure 1). The criteria also included flared iliac wings, flat acetabula and supra-acetabular notches in combination and dumbbell- or halberd-shaped metaphyseal widening of the long bones, particularly in the femora (figure 1). Other manifestations, including metaphyseal irregularities, epiphysial dysplasia, brachydactyly and delayed carpal bone age, were considered; however, these findings only partially contributed to the diagnosis because they were age-dependent and difficult to evaluate in younger patients.

The criteria for SMDK included a variable degree of platyspondyly (according to the age), overfaced pedicles, flat acetabula with/without flared iliac wings and supra-acetabular notches, flared metaphyses of the long bones without dumbbell shape, metaphyseal irregularities with almost normal epiphyses and almost normal short tubular bones (figure 2). Metaphyseal irregularities were assessable only in pre-pubertal patients. Carpal age was evaluated because delayed bone age has been emphasised as an essential finding of SMDK. BO was defined as the condition

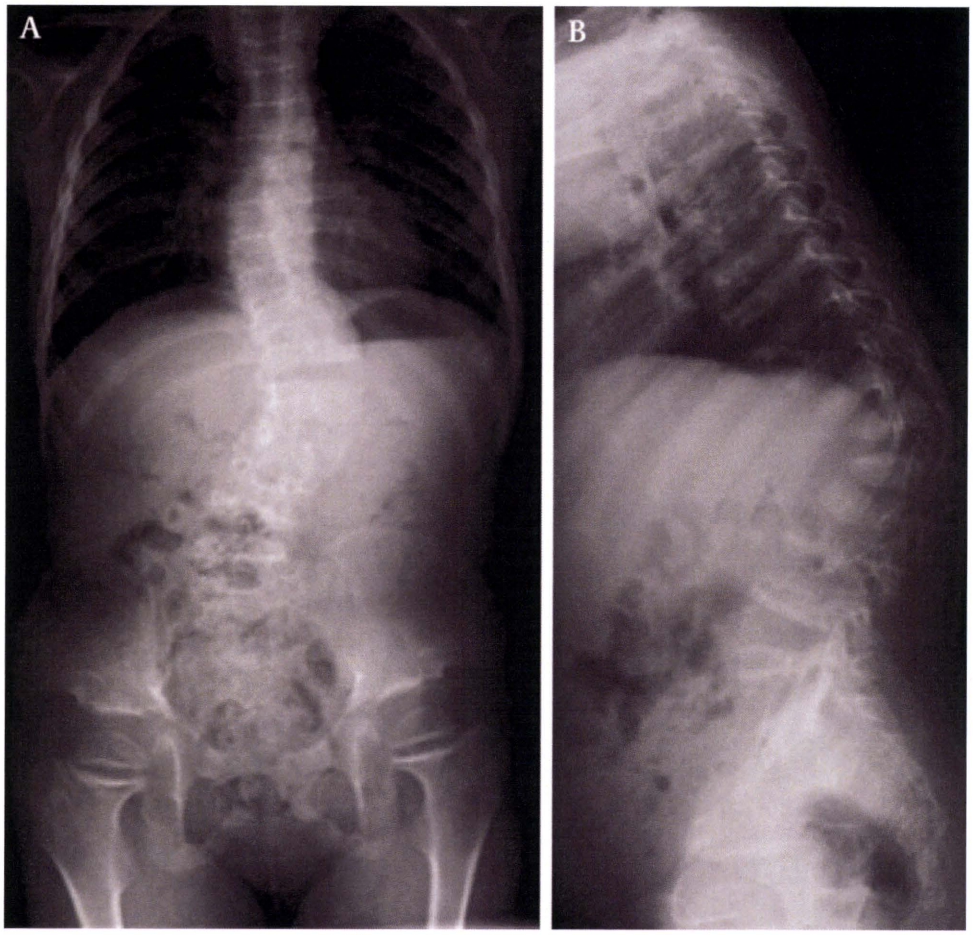

Figure 2 Radiographs of spondylometaphyseal dysplasia, Kozlowski type (SMDK) (S6). (A) AP and (B) lateral views of trunk at age 5 years and 9 months. Thoracolumbar kyphoscoliosis, platyspondyly with overfaced pedicles, flared ilia with supraacetabular notches are identical with those of metatropic dysplasia. However, mild flaring of the long bones contrasts with dumbbell deformity seen in metatropic dysplasia. Note metaphyseal dysplasia of the proximal femora. This patient had the common SMDK mutation, R594H.

that showed platyspondyly with overfaced pedicles and broad ilia, but no overt metaphyseal changes (flaring and irregularity).

Mutation search

Genomic DNA was extracted by standard procedures from peripheral blood or by Isohair kit (NIPPON GENE, Wako, Japan) from nail and hair. Exon sequence of *TRPV4* with its flanking intron sequence was amplified by PCR from genomic DNA. PCR products were sequenced directly by using an ABI Prism 3700 automated sequencer (PE Biosystems, Foster City, CA, USA). PCR primer sequence is available on request, and the same primer was used for sequencing. For confirmation of novel

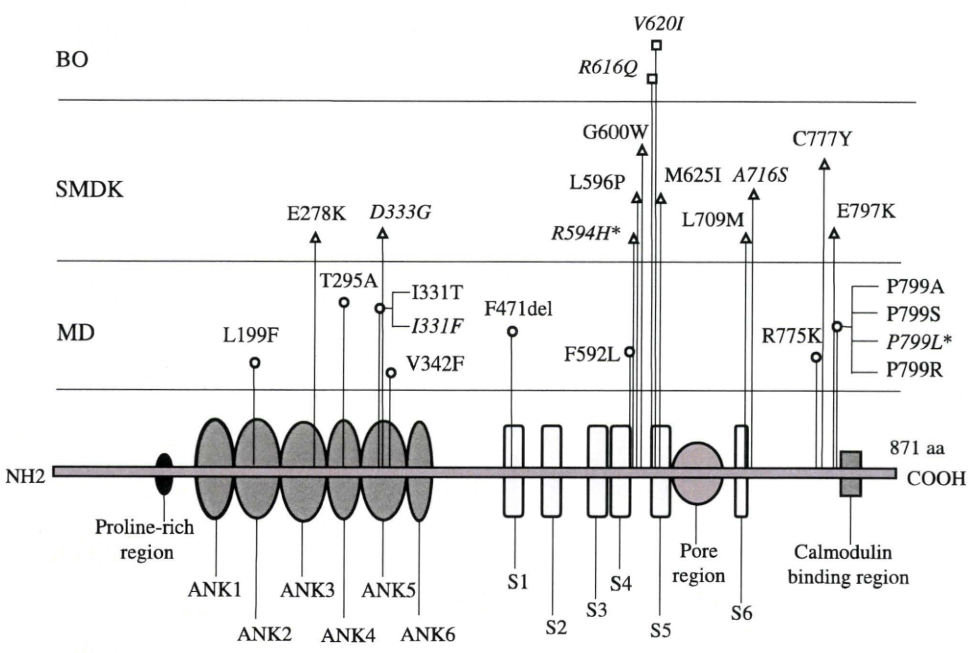

Figure 3 A diagram of human TRPV4 protein and location of mutations. ANK: ankyrin repeat region. S1–S6: transmembrane regions 1–6. BO: brachyolmia. SMDK: spondylometapyyseal dysplasia, Kozlowski type. MD: metatropic dysplasia. *Common recurrent mutations. Mutations found in the previous studies are in italic.

J Med Genet 2010;**47**:704–709. doi:10.1136/jmg.2009.075358

mutations in sporadic cases, genomic DNA from the unaffected parents was sequenced for the corresponding regions when parents' samples were available. The molecular analysis was performed independently in the two laboratories in Tokyo and in Freiburg.

Restriction fragment length polymorphism

PCR-restriction fragment length polymorphism (RFLP) method was used to confirm mutations in two hotspot codons, R594 and P799. c.1781G→A creates the *NcoI* (TAKARA BIO, Dalian, China) restriction site, and c.2395C→T/G and c.2396C→T/G abolishes *SmaI* (TAKARA BIO) restriction site, respectively. PCRs were the same as those for sequencing. We prepared the reaction mixture according to the manufactures of the two enzymes and incubated it at 37°C overnight. Digested PCR products were electrophoresed in 4% agarose gel (3% NuSieve GTG Agarose (Lonza, Rockland, Maine, USA) and 1% SeaKem LE Agarose (BMA, Rockland, Maine, USA)).

RESULTS

A total of 42 probands were included in the study. There were 14 Koreans, 14 Europeans, 10 Japanese, two Turks and one Indian. All MD cases were sporadic and four SMDK cases were familial. All were from non-consanguineous marriages. The clinical and radiological findings of the patients are summarised in supplementary tables 1 and 2. The phenotypes comprised 22 MD and 20 SMDK. In general, a radiological diagnosis of bone dysplasias rests on the overall pattern recognition of skeletal changes rather than a single radiological sign; after all, however, presence/absence of dumbbell- or halberd-shaped femora ascertained distinction between MD and SMDK (supplementary table 2). Other radiological signs were shared by both disorders. All subjects had flat acetabular roofs. Two SMDK patients (S12 and S18) did not show overt metaphyseal changes (Supplementary figure 1) and were considered to be of intermediate severity between SMDK and BO. Kozlowski *et al* (1982) reported SMDK with subtle metaphyseal irregularity.[4] All other subjects had metaphyseal changes (flaring and/or irregularity) (supplementary table 2).

Detailed radiographic review revealed several unexpected findings. Narrow thorax, prominent joints and coccygeal tail are considered to be clinical hallmarks of MD; however, only prominent joints were consistently found in MD, and these features were also occasionally found in SMDK (supplementary table 1). Evolution of body proportion with age, another hallmark of MD, was not essential; several post-pubertal MD patients showed short limbs, not short trunks. Delayed carpal age, a diagnostic criterion for SMDK, was not observed in half of SMDK patients. MD patients after infancy showed overfaced pedicles that were indistinguishable from those in SMDK patients. A small percentage of SMDK patients showed mild brachydactyly or mild epiphysial dysplasia/premature degenerative joint disease, yet, these cases were classified as SMDK based on the overall pattern of skeletal changes.

Mutations were found in 41 subjects (supplementary table 3). All subjects were at the heterozygous state for the mutation. We found 19 different *TRPV4* mutations; 17 were novel. All but c.1411_1413delTTC (p.F471del) were missense mutations, and all affected evolutionally conserved amino acids. We examined *TRPV4* sequences in the parents of probands with novel mutations except for S15, and confirmed that mutations in sporadic cases were all *de novo*. In S15, the mother's DNA was unavailable, but the mutation, c.1787T→C (p.L596P), was not found in the father, nor in 80 unrelated ethnicity-matched controls. L596 is highly conserved between diverse species (supplementary figure 2) and the observed amino-acid change is non-conservative. In two familial cases (S16 and S18) where their mutations were not proven to be *de novo* in this and previous studies, the substituted amino acids were also highly conserved among diverse species (supplementary figure 2). An *in silico* analysis by PANTHER (http://www.pantherdb.org/) indicated mutations as probably damaging protein function. There were no inconsistencies in segregation of the mutations in the family members as far as we examined.

Eleven different mutations were detected in 21 MD patients (supplementary table 3). One recurrent mutation, c.2396C→T (p.P799L), was detected in nine patients. It was confirmed as *de novo* in one family. Ten kinds of novel mutations were found. Eight of them were found only once; c.2324G→A (p.R775K) and c.2396C→G (p.P799R) were both found in two patients. Mutations altering codon 799 were detected in 13 patients. In M22, no mutation was found in the coding region of *TRPV4*, 5′- and 3′-UTRs, nor flanking intron sequences.

Eight different *TRPV4* mutations were found in SMDK (supplementary table 3). All 20 SMDK patients had heterozygous mutations in *TRPV4*; 14/20 mutations were in exon 11. A recurrent mutation, c.1781G→A (p.R594H) was found in 12 patients. The mutation was not found in normal parents in two families, indicating that they were *de novo*. The patients who showed intermediate phenotypes of SMDK and BO had the recurrent mutation, c.1781G→A and a novel mutation, c.2125C→A, respectively.

DISCUSSION

We found that *TRPV4* mutations in the MD and SMDK-disease spectrum include two mutational hotspots. We have observed the recurrent mutation c.1781G→A, which had been found in four SMDK patients in the previous study[12] and in 12 SMDK subjects in our cohort (supplementary table 3). The mutation was identified in various ethnic backgrounds. c.1781G→A is at present the most prevalent *TRPV4* mutation; 16/51 known cases carry this mutation. We also found that c.2396C→T is a recurrent mutation in MD (supplementary table 3). This mutation, found in one MD patient in the previous study,[11] was found in nine MD subjects with various ethnicities in our study. Knowledge of the mutation hot spots will enable the construction of an efficient screening system for *TRPV4* mutations and facilitate the molecular diagnosis of these diseases. The two RFLPs established in this study are useful tools for the screening of *TRPV4* mutations as they can capture ~60% (30/51) of *TRPV4* mutations.[11 12]

MD and SMDK mutations are clustered in specific exons. Exon 11 is a hot exon for SMDK mutations. 15 mutations were identified in this exon in our patient population and taken together with results of previous studies,[11 12] ~70% (18/26) of SMDK mutations were found in this exon. Only one exon-11 mutation has been identified in a MD patient. In contrast, exon 15 is a hot exon for MD mutations; ~60% (14/23) of MD mutations were found in this exon. There is only one exon-15 mutation in SMDK. All but one exon-15 mutation occurred at the same P799 codon; interestingly, four different mutations, leading to four different amino acid substitutions, were found at this "hot codon". In practice, these observations mean that we can prioritise specific *TRPV4* exons for MD and SMDK when searching for mutations. The locations of the mutations relative to the domains of the molecule (ANK, TM, cytoplasmic, etc.) did not show any consistent relation with phenotypes (figure 3).[13]

Despite genetic homogeneity of SMDK, its phenotypic range was broad, particularly in the severity of metaphyseal dysplasia and in appearances of ilia. The variable phenotypes, even due to the same mutation, are in part attributable to age-related differences. Sequential radiological follow-up would address this issue. MD patients who had mutations in exon 15 showed milder radiographic changes in terms of rib shortening, platyspondyly and dumbbell deformity than those with mutations in other exons (figure 1 and supplementary figure 3). However, accurate delineation of the total phenotypic spectrum even among individuals with the common mutation would require further accumulation of cases with radiographs taken at standard ages.

Genetic heterogeneity of MD has long been in debate. Most investigators have believed that MD comprises lethal autosomal recessive and non-lethal autosomal dominant phenotypes.[3] On the other hand, other investigators have suggested that all cases represent a dominant form with phenotypic variability.[2 14] Our series of patients included individuals with a relatively mild SMDK/BO phenotype and individuals with quite severe, though non-lethal, MD; thus, the concept that all forms of MD may be the result of dominant mutations seems quite likely. We studied one MD patient (M22) who did not have a *TRPV4* mutation. The girl, unlike other affected children, has not shown epiphysial dysplasia until now (supplementary figure 4). However, because she is still young, we have to follow-up her radiological evolution to determine whether her phenotype differs from those of other patients with *TRPV4* mutations (supplementary tables 1 and 2).

One MD patient had a 3-bp deletion in *TRPV4*. All other mutations in this study, as well as the seven mutations previously reported, are missense mutations.[11 12] The deletion mutation caused the loss of an evolutionally conserved amino-acid residue. From a previous functional study,[11] the molecular pathogenetic basis of TRPV4-pathies has been suggested to be a gain-of-function characterised by increased constitutive activity and elevated channel activation by a variety of mechanisms. It remains to be examined whether the deletion mutation would also cause a gain of TRPV4 function.

In summary, we found *TRPV4* mutations in 41 of 42 patients with MD and SMDK, indicating genetic homogeneity for these disorders. We identified 17 different novel mutations, including the first deletion mutation of *TRPV4*. We confirmed that R594H is a common and recurrent mutation in SMDK and found that P799L is a common and recurrent mutation in MD. There were mutational hot spots for *TRPV4*: R594 in exon 11 is a hot spot exclusive for SMDK mutations, while P799 in exon 15 is a hot spot for MD mutations. Our study presented an initial picture for the *TRPV4* mutation spectrum in MD and SMDK. Further studies are necessary to determine its complete picture and phenotypic extension of the *TRPV4* mutation.

Key points

- ***TRPV4* mutations were found in 40/41 subjects with MD and SMDK, including 17 kinds of novel mutations.**
- **Two mutation hot spots were identified for MD and SMDK, respectively.**
- **MD mutations were clustered at P799 in exon 15, while SMDK mutations were clustered at R594 in exon 11.**
- **Novel type of mutation other than missense mutation, 3-bp deletion was found in one MD patient.**
- **Our results would help diagnostic laboratories establish efficient screening strategies for genetic diagnosis of the *TRPV4* dysplasia family diseases.**

Author affiliations
[1]Laboratory for Bone and Joint Diseases, Center for Genomic Medicine, Tokyo, Japan
[2]The Center of Diagnosis and Treatment for Joint Disease, Drum Tower Hospital Affiliated to Medical School of Nanjing University, Nanjing, China
[3]Department of Radiology, Ajou University Hospital, Suwon, Korea
[4]Department of Orthopaedic Surgery, Seoul National University Children's Hospital, Seoul, Korea
[5]Centre for Pediatrics and Adolescent Medicine, University of Freiburg, Freiburg, Germany
[6]Department of Pediatrics and Medical Genetics Section, Tenshi Hospital, Sapporo, Japan
[7]Department of Paediatric Orthopedics, Shizuoka Children's Hospital, Shizuoka, Japan
[8]Department of Rehabilitation Medicine, Graduate School of Medicine, The University of Tokyo, Tokyo, Japan
[9]Department of Spine Surgery, Yokohama Rosai Hospital, Yokohama, Japan
[10]Department of Orthopaedic Surgery, Nagoya University School of Medicine, Nagoya, Japan
[11]Department of Orthopaedic Surgery, Korea University Guro Hospital, Seoul, Korea
[12]Department of Pediatrics, Samsung Medical Center, Seoul, Korea
[13]Department of Orthopaedic Surgery, Pusan National University Hospital, Pusan, Korea
[14]Department of Pediatrics, School of Medicine, Sapporo Medical University, Sapporo, Japan
[15]Neonatal Intensive Care Unit, Ospedali Riuniti, Bergamo, Italy
[16]Clinical Genetics, Karolinska University Hospital, Solna, Stockholm, Sweden
[17]Department of Pediatric Genetics, Amrita Institute of Medical Sciences & Research Centre, AIMS Ponekkara PO, Cochin, Kerala, India
[18]Department of Pediatrics, Graduate School of Medicine, Chiba University, Chiba, Japan
[19]Department of Pediatrics, National Hospital Organization, Kure Medical Center, Kure, Japan
[20]Department of Pediatrics, Graduate School of Medicine, Gifu University, Gifu, Japan
[21]Department of Clinical Genetics, 849 Antropogenetica, Radboud University Medical Centre, Nijmegen, The Netherlands
[22]Department of Pediatric Genetics, Emma Childrens' Hospital/Academic Medical Center, Amsterdam, The Netherlands
[23]Department of Pediatrics, Academic Medical Center, University of Amsterdam, AZ Amsterdam, The Netherlands
[24]Clinical Genetic Unit, Department of Obstetrics and Pediatrics, Fondazione Ospedale Maggiore Policlinico Mangiagalli e Regina Elena, Milano, Italy
[25]Department of Clinical Genetics, Oulu University Hospital, Oulu, Oys, Finland
[26]Division of Medical Genetics, Saitama Children's Medical Center, Iwatsuki, Japan
[27]Department of Radiology, Tokyo Metropolitan Kiyose Children's Hospital, Kiyose, Japan

Acknowledgements We are grateful to patients, their family members and their doctors for participating in the study. We also thank Dr Yasemin Alanay for help given to our study in patient collection. This project was supported by Grants-in-aids from the Ministry of Education, Culture, Sports and Science of Japan (Contract grant No. 20390408), from Research on Child Health and Development (Contract grant No. 20-S-3) and from the Korea Healthcare technology R&D Project, Ministry for Health, Welfare and Family Affairs, Republic of Korea (No. A080588). This project was also supported by the European Skeletal Dysplasia Network (ESDN; http://www.esdn.org), as well as the Japanese Skeletal Dysplasia Consortium (JSDC; http://www.riken.jp/lab-www/OA-team/JSDC/), by grants from the German Ministry for Education and Research (BMBF contract grant "SKELNET") and by the European Union (FP6, Contract grant "EuroGrow"), and by the University of Freiburg. E.L. and B.Z. are supported by individual grants from Deutsche Forschungsgemeinschaft (La 1381/1-3).

Funding Grants-in-aids from the Ministry of Education, Culture, Sports and Science of Japan; Research on Child Health and Development; Korea Healthcare technology R&D Project, Ministry for Health, Welfare and Family Affairs, Republic of Korea; European Skeletal Dysplasia Network (ESDN; www.esdn.org); Japanese Skeletal Dysplasia Consortium (JSDC; http://www.riken.jp/lab-www/OA-team/JSDC/); German Ministry for Education and Research (BMBF contract grant "SKELNET"); European Union (FP6, Contract grant "EuroGrow"); University of Freiburg; Deutsche Forschungsgemeinschaft.

Competing interests None.

Patient consent Obtained.

Ethics approval This study was conducted with the approval of the Ethical Committee of RIKEN, Japan.

Contributors Jin Dai, Ok-Hwa Kim, and Tae-Joon Cho, these authors are contributed equally to the work.